DOI: 10.1002/ejic.200600921

Mechanistic Studies on the Activation of NO by Iron and Cobalt Complexes

Alicja Franke,[a] Federico Roncaroli,[a,b] and Rudi van Eldik*[a]

Keywords: Activation of NO / Reductive nitrosylation / Kinetics / Cytochrome P450 / Vitamin B_{12} / Porphyrins / Chelates

In this review, the reactions of nitric oxide with selected Fe and Co complexes of biological and environmental importance are reviewed. Fundamental chemical kinetics and mechanisms of reactions that lead to the formation and decay of nitrosyl complexes are illustrated and discussed on the basis of studies on Fe^{II} chelates, $Fe^{II/III}$ pentacyano complexes, Fe^{III} porphyrins, cytochrome P450 and model complexes, $Co^{II/III}$ porphyrins and vitamin B_{12}. Throughout the review, the focus is on mechanistic details of the binding of NO to and the release of NO from metal complexes and on the nature of the stable metal–NO complexes produced in solution. As will be seen for most of the presented reactions, the interaction of NO with the metal complex involves activation of the small NO molecule so that charge transfer occurs as a result of the formation of the metal–NO bond.

[a] Institute for Inorganic Chemistry, University of Erlangen-Nürnberg,
Egerlandstr. 1, 91058 Erlangen, Germany
E-mail: vaneldik@chemie.uni-erlangen.de
[b] Department of Inorganic, Analytical and Physical Chemistry, INQUIMAE, Faculty of Exact and Natural Sciences, University of Buenos Aires,
C1428EHA Buenos Aires, Argentina

1. Introduction

In recent years, we developed an interest in the interaction of NO with complexes of Fe, Co and Ru, and in their mechanistic understanding. Since this was a new research area for us, we were confronted with many fundamental questions that forced us to make a critical evaluation of the

Alicja Franke was born in Biecz, a small town in south-eastern Poland, in 1972. After completing her M.Sc. in 1996 from the Jagiellonian University, Krakow, she was awarded TEMPUS (1997) and DAAD (1998) Fellowships to perform research work at the University of Erlangen-Nürnberg, Germany, in the group of Prof. Rudi van Eldik. In 2001 she received her PhD in the kinetics and mechanism of nitric oxide donation and binding in model systems of biological relevance, under the supervision of Prof. Grazyna Stochel (Jagiellonian University). In 2002 she joined the research group of Prof. Rudi van Eldik as a post-doctoral fellow. She continues to work in Erlangen on the kinetics and mechanism of small-molecule activation by iron-heme centres, as well as on the activation of organic peracids by cytochrome P450 and model complexes in the "peroxide-shunt" catalytic cycle.

Federico Roncaroli was born in Buenos Aires, Argentina, in 1976. He graduated as a chemist in 2000 at the University of Buenos Aires. In 2001 he was awarded a doctoral fellowship from the Scientific Research Council of Argentina (CONICET) to perform research work at the University of Buenos Aires and at the University of Erlangen-Nürnberg, Germany. At the first institution, he studied the reactivity and spectroscopic properties of metal–nitrosyl complexes under the direction of Professor José Olabe, which allowed him to earn a PhD degree in 2004. At the second institution, under the supervision of Professor Rudi van Eldik, his work focused on the reactions of nitric oxide with biologically relevant complexes like vitamin B_{12} and metal porphyrins, for which he was awarded a Dr. rer. nat. in 2005. His current interests are bioinorganic chemistry, homogeneous catalysis and activation of small molecules.

Rudi van Eldik was born in 1945 in Amsterdam and grew up in Johannesburg (South Africa). He received his chemistry education and Ph.D. at Potchefstroom University (SA), followed by post-doctoral work with Gordon M. Harris (SUNY at Buffalo, NY) and Hartwig Kelm (University of Frankfurt, Germany). After completing his habilitation in physical chemistry at the University of Frankfurt in 1982, he was appointed as Professor of Inorganic Chemistry at the private University of Witten/Herdecke in 1987. In 1994 he accepted his present position as Professor of Inorganic and Analytical Chemistry at the University of Erlangen-Nürnberg. His research interests cover the elucidation of inorganic, organometallic and bioinorganic reaction mechanisms, with special emphasis on the application of high-pressure thermodynamic and kinetic techniques. He is presently editor of Advances in Inorganic Chemistry and author of ca. 680 research papers and reviews in international journals (www.chemie.uni-erlangen.de/vaneldik). He has developed a promotional activity for chemistry and related experimental sciences in the form of chemistry edutainment over the past ten years (www.magic-chemistry-lecture.com).

existing literature data at that time. One aspect that was particularly disturbing was the fact that for many metal–NO complexes the exact oxidation state of both components was not stated and the Enemark and Feltham notation[1] was adopted in which the product is written as $\{M–NO\}^{(n+1)}$, where n represents the number of d electrons of the metal ion [one is added (n + 1) for the unpaired electron on the NO radical]. From a basic coordination chemistry viewpoint, this situation was not very satisfying since the oxidation state of the metal centre is very crucial for the understanding of its chemical behaviour and for analysing the extent to which the coordinated NO is 'activated' during the binding process. Another aspect that caused us to run into severe problems was the fact that in aqueous solutions of NO there are always unavoidable traces of nitrite that can totally inhibit or overrule the reaction with NO. Thus, we wondered whether it is really NO that reacts under the selected conditions, and if it is NO, what is the nature of the M–NO complex that is formed in terms of the formal-oxidation-state assignment. Along these lines, the first review of our work was entitled: 'To be or not to be NO in coordination chemistry? A mechanistic approach'.[2]

In this microreview, we focus on our most recent mechanistic studies dealing with the interaction of NO with complexes of Fe^{II}, Fe^{III}, Co^{II} and Co^{III}, which also include the enzymes cytochrome P450 and vitamin B_{12}, as well as suitable model systems. The interaction will describe the reversible binding kinetics of NO, the characterization of the produced metal–nitrosyl complex, and provide information on subsequent reactions that lead to stable product species. The employed kinetic techniques (stopped-flow and laser flash photolysis at ambient and high pressure) allowed the extraction of the appropriate rate constants and activation parameters for the forward ("on") and back ("off") reactions for the reversible binding of NO and enabled us to discuss mechanisms underlying NO-substitution processes. In general, substitution reactions involving the displacement of a ligand coordinated to a metal centre by a free ligand in solution can be visualized as presented schematically in Figure 1.

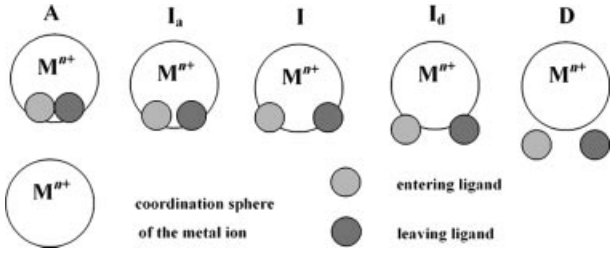

Figure 1. Schematic representation of the transition states of different substitution mechanisms.

If the activation parameters for the "on" and "off" reactions support an intermediate of higher and lower coordination number than in the reactant state, the mechanisms are of the limiting type denoted as associative (A) and dissociative (D), respectively. When the association and dissociation of the entering and leaving ligand, respectively, occur to an equal extent, then the mechanism can be described as an interchange (I) process. However, a "pure" interchange mechanism occurs very rarely and more often associative interchange (I_a) and dissociative interchange (I_d) mechanisms are observed in which the entering and leaving ligands are either firmly (I_a) or weakly (I_d) embedded in the coordination sphere of the metal ion.

2. Structure and Properties of Metal Nitrosyls

Binding of NO to a metal centre must result in the stabilisation of NO, a radical species in the ground state. Such stabilisation can be achieved by a shift of electron density to the metal centre or to the nitrosyl ligand and can formally be described as the formation of the nitrosyl cation (NO^+) or the nitroxyl anion ($NO^–$), respectively, as depicted by the mesomeric structures in reactions (1a) and (1b).

$$(L)M^{n+} + NO \rightleftharpoons (L)M^{n+}–NO \leftrightarrow (L)M^{(n-1)+}–NO^+;$$
linear M–N–O group (1a)

$$(L)M^{n+} + NO \rightleftharpoons (L)M^{n+}–NO \leftrightarrow (L)M^{(n+1)+}–NO^–;$$
bent M–N–O group (1b)

In reaction (1a), the NO^+ group is isoelectronic with CO, whereas in reaction (1b) the $NO^–$ group is isoelectronic with O_2. These two formal descriptions of the M–N–O bond are extreme and ideal, since metal–nitrosyl complexes usually show M–NO angles between 180° and 120°, and their electronic structures cannot be described as $M–NO^+$ or $M–NO^–$. Moreover, some complexes can be described as $(L)M^{n+}–NO^{\cdot}$, where the odd electron is *mainly* located on the metal. Nevertheless, in terms of the coordination chemistry at hand, it is in many cases useful to think in terms of formal oxidation states in order to understand the mechanistic behaviour of the complexes. A detailed account of the formal description of these limiting situations along with the description introduced by Enemark and Feltham have been published in an earlier account from our group.[2] The characterization of the produced metal–nitrosyl complexes has, in general, been done on the basis of EXAFS, XAS Fe-edge, resonance Raman, EPR and Mössbauer spectroscopic and magnetic circular dichroism data. Spin-crossover and spin-coupling phenomena account for the overall observed spin behaviour of the investigated complexes.

3. Interaction of NO with Fe^{II} Chelate Complexes

Before we discuss the results of the interaction of NO with Fe^{II} chelate complexes, we would like to refer to the interaction of NO with aquated Fe^{II} in acidic medium, a classical text book example that forms part of the well-known brown-ring test for nitrate. A detailed kinetic and spectroscopic study[3] revealed that the overall reaction can be formulated as shown in reaction (2), where the product is formally an $Fe^{III}–NO^–$ species in which the high-spin Fe^{III} (S = 5/2) is antiferromagnetically coupled to the two un-

paired electrons on NO^- ($S = 1$) to result in the overall $S = 3/2$ spin state of the product.

$$[Fe^{II}(H_2O)_6]^{2+} + NO \underset{k_{off}}{\overset{k_{on}}{\rightleftharpoons}} [Fe^{III}(H_2O)_5(NO^-)]^{2+} + H_2O \quad (2)$$

The 'on' reaction is controlled by water exchange on $[Fe(H_2O)_6]^{2+}$ and follows an I_d mechanism as can be clearly seen from the volume profile for this reaction reported in Figure 2.

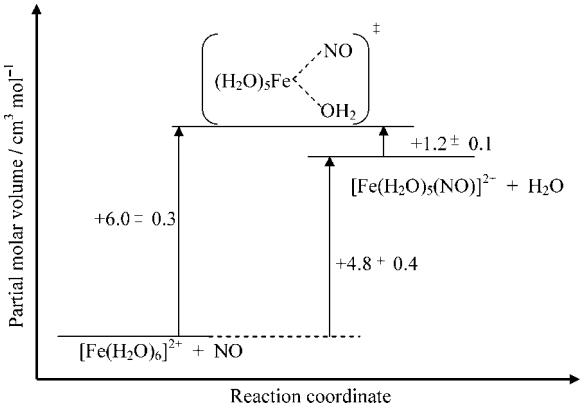

Figure 2. Volume profile for the binding of NO to aquated Fe^{II} as given in reaction (2).[3]

The introduction of a chelate such as a polyaminocarboxylate labilizes the Fe^{II} complex and significantly increases the water-exchange rate constant. The nitrosation of such complexes can be formulated as shown in reaction (3). Spectroscopic data suggested that the reaction product is formally Fe^{III}–NO^-.

$$[Fe^{II}L(H_2O)]^{2+} + NO \underset{k_{off}}{\overset{k_{on}}{\rightleftharpoons}} [Fe^{II}L(NO)]^{2+} + H_2O \quad (3)$$

A systematic study of the series of $Fe^{II}(L)$ complexes with different polyaminocarboxylate ligands indicated that their ability to reversibly bind NO is strongly affected by the selected chelating ligand. This influence is apparent from the large variation in the overall binding constant K_{NO} ($= k_{on}/k_{off}$), which spans a wide range from ca. 1×10^3 to 2×10^7 M^{-1} for the studied complexes (see Figure 3).[4] In addition, an interesting correlation was found between the stability of the $Fe^{III}(L)(NO^-)$ complexes and the oxygen sensitivity of the parent $Fe^{II}(L)$ complexes, in other words, their tendency to form $Fe^{III}(L)(O_2^-)$ species. From the comparison presented in Figure 3, it can, in general, be concluded that the higher the K_{NO} value for a given metal–nitrosyl complex, the larger the oxygen sensitivity of the parent $Fe^{II}(L)$ complex. Clearly, an increasing inductive effect of the chelate ligand causes an increase in stability of the Fe^{III}–NO^- bond and also an enhancement of the shift of electron density from iron to oxygen atom in the corresponding $Fe^{III}(L)(O_2^-)$ complex.

A quantitative basis for the observed trends in the stability of the $Fe^{III}(L)(NO^-)$ complexes was provided by kinetic and mechanistic studies on the binding and release of NO from selected $Fe^{II}(L)$ complexes. The complexes exhib-

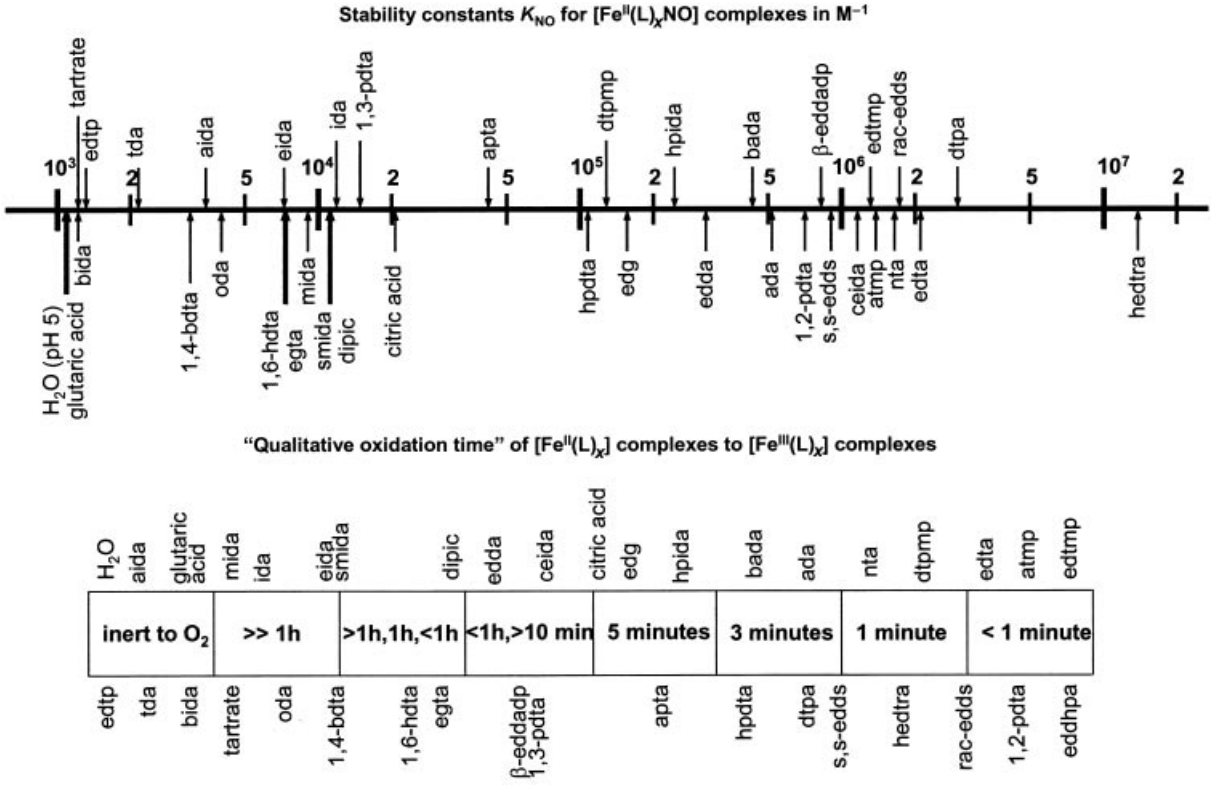

Figure 3. Correlation between K_{NO} [defined by reaction (3)] and qualitative oxidation time of selected $Fe^{II}(L)$ complexes.[4]

ited quite different behaviour in their reactions with NO. The observed differences are particularly large in the case of the Fe^{II}(mida) and Fe^{II}(edta) complexes: the mida complex shows almost no oxygen sensitivity, exhibits a low binding affinity for NO and releases NO almost completely on passing an inert gas through the solution. In contrast, the edta complex is extremely oxygen sensitive, shows a very high binding affinity for NO and releases NO only slowly when treated with an inert gas.

More detailed insight into the mechanisms of the thermal reactions in which NO binds and dissociates from the iron centre in the studied Fe^{II}(L) systems comes from activation parameters for the "on" and "off" reactions, obtained from systematic studies of k_{on} and k_{off} as a function of temperature and pressure.[5] The positive volumes of activation found in most cases clearly indicate that the complex-formation reactions can be best described by a dissociative interchange (I_d) mechanism. The exception is the reaction of Fe^{II}(nta)$(H_2O)_2$ with NO, which exhibits a definite (Figure 4) negative volume of activation, suggesting that the reaction occurs through an associative interchange (I_a) mechanism. The difference in the mechanism of nitrosylation observed for the Fe^{II}(nta)$(H_2O)_2$ complex relative to the other studied complexes becomes clear from a comparison of the volume profiles for the edta and nta systems shown in Figure 4. Such a variation in the mechanism presumably reflects the fact that Fe^{II}(nta)$(H_2O)_2$ is a six-coordinate complex, whereas it is known that Fe^{II}(edta)H_2O is seven-coordinate. This would mean that some complexes react according to an I_d mechanism as a result of their seven-coordinate, 20-valence-electron character, whereas the six-coordinate nta complex reacts according to an I_a mechanism because of its 18-valence-electron character. These results suggest that water-exchange reactions on the studied Fe^{II}(L) complexes presumably control the kinetics and mechanism of the NO binding.

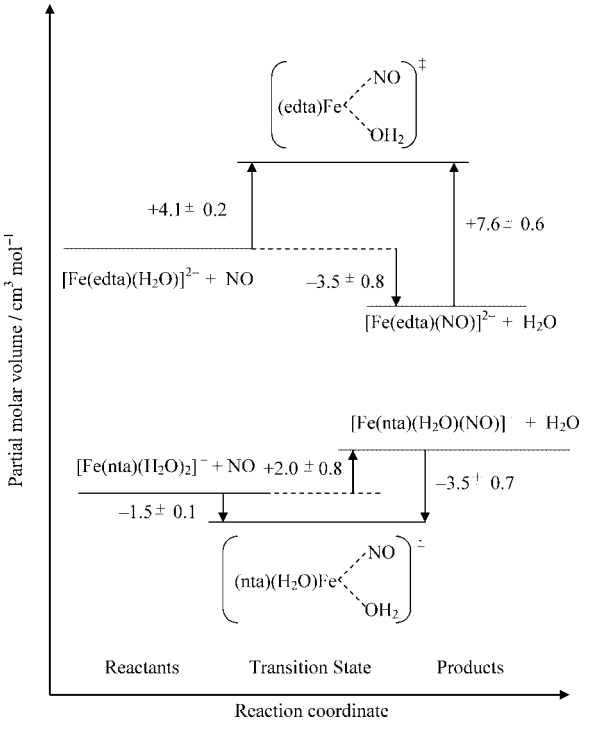

Figure 4. Volume profiles for the reversible binding of NO to $[Fe^{II}(edta)H_2O]^{2-}$ (top) and $[Fe^{II}(nta)(H_2O)_2]^{-}$ (bottom).[5]

4. Interaction of NO with Pentacyanoferrate(II)

Complex-formation and -dissociation reactions of the $[Fe^{II}(CN)_5(H_2O)]^{3-}$ complex have been extensively studied over the past decades for a good variety of ligands.[6,7] For this reason, this complex seemed to be an attractive choice for studying the reaction with NO and for comparing its binding, reactivity and coordination properties with other ligands; a comparison which, to the best of our knowledge, was missing or not addressed thoroughly enough in the literature. In this way, the investigated reaction is shown in reaction (4).

$$[Fe^{II}(CN)_5(H_2O)]^{3-} + NO \rightleftharpoons [Fe^{II}(CN)_5(NO^{\cdot})]^{3-} + H_2O;\ k_f,\ k_d \quad (4)$$

The product of reaction (4), the $[Fe^{II}(CN)_5(NO^{\cdot})]^{3-}$ complex, which can also be generated upon reduction of nitroprusside with several reducing agents or with different techniques (i.e. electrochemical, pulse radiolysis),[8,9] was characterized by different spectroscopic methods (UV/Vis, IR, EPR).[8,9] This compound was postulated to be responsible for the hypotensive effect of nitroprusside, i.e. $[Fe^{II}(CN)_5(NO^{+})]^{2-}$ is reduced in biological fluids to the $[Fe^{II}(CN)_5(NO^{\cdot})]^{3-}$ complex, which eventually releases NO.[10] This complex shows a *trans*-labilization effect which can be formulated as shown in reaction (5).

$$[Fe^{II}(CN)_5(NO^{\cdot})]^{3-} \rightleftharpoons [Fe^{I}(CN)_4(NO^{+})]^{2-} + CN^{-};\ k_5,\ k_{-5},\ K_5 \quad (5)$$

The parameters of reaction (5) were determined at 25 °C: $k_5 = 2.7 \times 10^2\ s^{-1}$, $k_{-5} = 4 \times 10^6\ M^{-1}\,s^{-1}$, $K_5 = 6.8 \times 10^{-5}$ M.[9] They indicate that the equilibrium is driven to the formation of the $[Fe^{II}(CN)_5(NO^{\cdot})]^{3-}$ species at high pH (>8) and in the presence of CN^-.

UV/Vis and EPR spectroscopic data at pH > 8 showed that the $[Fe^{II}(CN)_5(NO^{\cdot})]^{3-}$ complex is the product of reaction (4).[11] Between pH 4 and 8, the $[Fe(CN)_5(NO)]^{3-}$ complex could not be detected, which is in agreement with reaction (5).[12] However, a systematic study of the reaction between $[Fe^{II}(CN)_5(H_2O)]^{3-}$ and NO as a function of the pH allowed us to conclude that the reaction is controlled by the substitution of the coordinated water molecule by NO, i.e. the decay of the $[Fe(CN)_5(H_2O)]^{3-}$ complex was independent of the pH (4–10).[11]

From a systematic study as a function of the NO concentration, the complex-formation rate constant $k_f = 250 \pm 10\ M^{-1}\,s^{-1}$ (25.4 °C, I = 0.1 M, pH = 7.0) was obtained. As shown in Table 1, this value is very close to the complex-formation rate constant for several neutral ligands. Experiments at different temperatures and pressures afforded the activation parameters $\Delta H^{\#} = 70 \pm 1\ kJ\,mol^{-1}$, $\Delta S^{\#} = +34 \pm 4\ J\,K^{-1}\,mol^{-1}$ and $\Delta V^{\#} = +17.4 \pm 0.3\ cm^3\,mol^{-1}$. In Table 1, the activation parameters are also compared with

the corresponding values for other ligands. Several mechanisms have been proposed to explain these complex-formation reactions (Scheme 1).

Table 1. Complex-formation rate constants and activation parameters for different $[Fe^{II}(CN)_5L]^{n-}$ complexes.[a]

Ligand	k_f [$M^{-1}s^{-1}$]	$\Delta H_f^{\#}$ [$kJ\,mol^{-1}$]	$\Delta S_f^{\#}$ [$J\,K^{-1}mol^{-1}$]	$\Delta V_f^{\#}$ [$cm^3\,mol^{-1}$]	Ref.
N-Mepz^{+}[b,c]	550[b]	70.3	+42		[7]
	2350[c]				[6]
CO[c]	310	63	+15		[7]
NO[c]	250	70	+34	+17.4	[11]
dmso[b]	240	64.4	+16.7		[7]
pz[d]	380	64.4	+20.9		[7]
his[c]	315	64.4	+21	+17.0	[7,14]
py[d]	365	67.4	+29.3		[7]
NH_3[c]	365	62	+10		[7]
	452	78	+67	+14.4	
Im[c]	242	63.5	+12.5	+15.5	[7,14]
CN^-[b]	30	76.9	+42	+13.5	[16]

[a] For the reaction: $[Fe(CN)_5H_2O]^{3-} + L \rightarrow [Fe(CN)_5L]^{n-} + H_2O$, T = 25.0 °C, with the exception of L = NO where T = 25.4 °C. [b] I = 1 M. [c] I = 0.1 M. [d] I = 0.5 M.

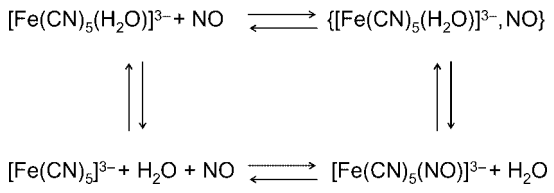

Scheme 1.

In the limiting dissociative mechanism (D), the reaction is controlled by the release of the water molecule, generating a pentacoordinate intermediate (left side of Scheme 1), followed by fast coordination of NO (bottom of Scheme 1).[13] The dissociative interchange mechanism (I_d) implies the rapid formation of a precursor complex between $[Fe(CN)_5(H_2O)]^{3-}$ and NO (top of Scheme 1), followed by the rate-determining ligand interchange between the first and the second coordination spheres of the precursor complex (right side of Scheme 1).[13] Finally, in a variation of the last mechanism (D_{pc}), the slow dissociation of the water molecule occurs within a precursor complex.[6] All of these mechanisms agree with the second-order behaviour of the rate law and with the dependence of k_f on the charge of the coordinating ligand. The consistent rate constants found for the complex-formation reactions with different ligands of the same charge, and the significantly large and positive values for the activation entropies and volumes, suggest the operation of a D mechanism.[13] An additional argument presented in favour of the D mechanism is based on the principle of microscopic reversibility, since strong evidence, i.e. large activation volumes, supports the operation of a D mechanism in the complex-dissociation reaction (k_d). Moreover, the activation volumes in Table 1 range from +14 to +18 $cm^3\,mol^{-1}$.[14] These values are consistent with the theoretical activation volume calculated for the dissociation of a water molecule in an octahedral metal centre (+13.1 $cm^3\,mol^{-1}$).[15]

From the complex-formation rate constants, we conclude that NO behaves like a normal Lewis base. Since the complex-formation rate constant is controlled by the dissociation of water, it is not possible to obtain specific information on the coordination properties of NO, and no specific influence of the unpaired electron on NO is observed when it is compared with the coordination ability of diamagnetic ligands.

The $[Fe(CN)_5(NO)]^{3-}$ complex is the product of reaction (4), and we were able to generate it through the reaction between $[Fe(CN)_5(H_2O)]^{3-}$ and NO at pH > 8. The addition of CN^- allowed us to prevent the formation of the $[Fe(CN)_4NO]^{2-}$ complex and its subsequent reactions.[12] In this way, it was possible to study the complex-dissociation reaction (k_d). The overall reaction of the former complex in the presence of CN^- is shown in reaction (6).

$$[Fe(CN)_5(NO)]^{3-} + CN^- \rightleftharpoons [Fe(CN)_6]^{4-} + NO \quad (6)$$

During reaction (6), the characteristic bands of the reactant at 347 and 440 nm decayed according to a first order process. Only a shoulder at 320 nm, assignable to $[Fe(CN)_6]^{4-}$, remained. NO was detected by mass spectrometry and electrochemical techniques.[11] With excess cyanide, the observed rate constant is independent of the concentration of this ligand, and reaction (6) is controlled by the dissociation of NO, i.e. k_d. At pH 10 (25.0 °C, I = 0.1 M), the observed rate constant was $(1.58 \pm 0.06) \times 10^{-5}\ s^{-1}$. The activation parameters were $\Delta H^{\#} = 106.4 \pm 0.8\ kJ\,mol^{-1}$, $\Delta S^{\#} = +20 \pm 2\ J\,K^{-1}mol^{-1}$ and $\Delta V^{\#} = +7.1 \pm 0.2\ cm^3\,mol^{-1}$. Table 2 summarizes the data for the complex-dissociation rate constants for similar complexes with different ligands that show different σ–π interactions with the metal centre. The activation enthalpies and entropies are consistent with those reported for the release of other ligands in the pentacyanoferrate(II) fragment. Although the activation volume for NO is significantly smaller than for other ligands, it is still indicative of a D mechanism. In Table 2, we can appreciate that k_d for NO is significantly lower than for most ligands, comparable to that for the π-acceptor ligand DMSO, but faster than those for the strong π-acceptor ligands such as CO, CN^- or NO^+ (the release of NO^+ is, in principle, undetectable in $M^{II}NO^+$ complexes).

In view of the presented value of k_d, we conclude that NO is not released from the $[Fe(CN)_5(NO)]^{3-}$ complex after biological reduction of nitroprusside. In vitro experiments showed that conditions favouring the release of CN^- after reduction of nitroprusside are required to allow the release of NO.[12] Figure 5 shows the volume profile for reaction (4) constructed with the activation volumes determined for k_f and k_d. Evidently, the partial molar volume of the transition state is much larger than that of the reactant and the product states, which is consistent with the proposal of a D mechanism. This mechanism is in agreement with that expected for a pentacyano fragment, where the σ-donor and π-acceptor properties of the ligands cause significant *trans*- and *cis* labilization of water or NO.[7]

Several volume profiles for the reversible binding of NO to different iron complexes have been recently reported,

Table 2. Dissociation rate constants and activation parameters for different $[Fe^{II}(CN)_5L]^{n-}$ complexes.[a]

Ligand	k_d [s^{-1}]	$\Delta H_d^{\#}$ [kJ mol^{-1}]	$\Delta S_d^{\#}$ [J K^{-1} mol^{-1}]	$\Delta V_d^{\#}$ [cm^3 mol^{-1}]	Ref.
CO[b,c]	$<10^{-8}$				[7]
CN^-[c,d]	ca.4×10^{-7}				[17]
NO[c]	1.58×10^{-5}	106.4 ± 0.8	$+20\pm2$	$+7.1\pm0.2$	[11]
dmso[c]	7.5×10^{-5}	110.0	+46.0		[7]
N-Mepz$^+$[e]	2.8×10^{-4}	115	+75	+0.9	[7,18]
pz[e]	4.2×10^{-4}	110.5	+58.6	+13.0	[7,18]
his[c]	5.3×10^{-4}	105.4	+46.0		[7]
2-Mepz[e]	7.7×10^{-4}	114	+44	+19.4	[19]
4-CNpy[e]	1×10^{-3}	105	+50	+20.6	[19]
py[e]	1.1×10^{-3}	103.8	+46.0		[7]
3,5-Me_2py[e]	1.2×10^{-3}	108	+60	+20.5	[7,20]
3-CNpy[e]	2.2×10^{-3}	93	+16	+20.6	[20]
NO_2^-[c]	1×10^{-2}	97	+42	+20.1	[21]
NH_3[c]	1.75×10^{-2}	102	+68	+16.4	[7]

[a] T = 25.0 °C. [b] Estimated number, measured using pz as a scavenger. [c] I = 0.1 M. [d] Extrapolated from data reported at higher temperatures. [e] I = 0.5 M.

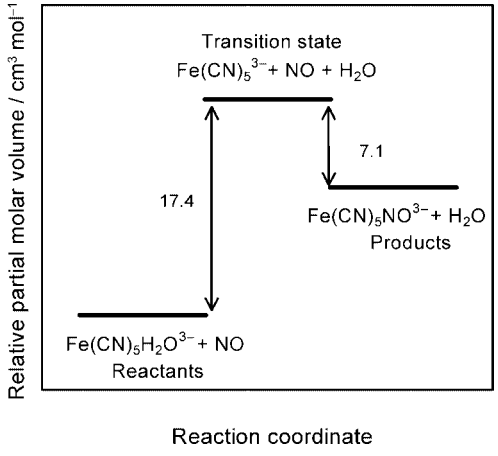

Figure 5. Volume profile for the overall reaction (4).

some of them support the operation of a D mechanism. Examples are the reaction of NO with metmyoglobin and some iron(III) porphyrin complexes. It is important to note that the volume profile shown in Figure 5 is the first reported for a reversible reaction with NO where no formal charge transfer occurs during the reaction, as is the case for the previously reported data.

5. Interaction of NO with Pentacyanoferrate(III)

The reaction between the $[Fe(CN)_5(H_2O)]^{2-}$ complex and NO produces quantitatively $[Fe(CN)_5NO]^{2-}$ (nitroprusside).[24] Thus, the overall reaction can be described by reaction (7) (k_f and k_d are redefined for this reaction).

$$[Fe^{III}(CN)_5(H_2O)]^{2-} + NO \rightleftharpoons [Fe^{II}(CN)_5(NO^+)]^{2-} + H_2O;\ k_f,\ k_d \quad (7)$$

Several attempts were made to determine k_d by using trapping agents for the released NO, but they were unsuccessful, probably due to the slowness of the release reaction. When the $[Fe(CN)_5(H_2O)]^{2-}$ complex reacted with excess NO, the characteristic bands of the reactant at 394 and 340 nm decayed and a new band at 264 nm, assignable to nitroprusside, grew following a first-order behaviour. By working at different NO concentrations, k_f was found to be 0.252 ± 0.004 M^{-1} s^{-1} (25.5 °C, I = 0.1 M). From the pressure and temperature dependence of reaction (7), the activation parameters were obtained: $\Delta H^{\#} = 52\pm1$ kJ mol^{-1}, $\Delta S^{\#} = -82\pm4$ J K^{-1} mol^{-1} and $\Delta V^{\#} = -13.9\pm0.5$ cm^3 mol^{-1}.[24]

Although the coordination chemistry of the pentacyanoferrate(III) system has not been disclosed as deeply as for the Fe^{II} analogue, there are studies with several other ligands that allow a comparison with our results for NO. In general, substitution reactions of this complex are slow reactions with second-order rate constants that range from 10^{-4} to 10^{-7} M^{-1} s^{-1}.[21–23] The activation entropies and volumes for the substitution reaction with some nucleosides were studied. The values were in the range 5–120 J K^{-1} mol^{-1} and 3–6 cm^3 mol^{-1}, respectively.[23] These data were interpreted in terms of a dissociative interchange mechanism (I_d) and proposed to be generally valid for water-substitution reactions of $[Fe(CN)_5(H_2O)]^{2-}$. These slow reactions can be catalyzed by Fe^{II} or other reducing species.[21,22]

In contrast, k_f is several orders of magnitude faster than the typical values for substitution reactions of this complex. Moreover, the activation entropy and volume are negative.[24] On the basis of these discrepancies, we propose that reaction (7) is controlled by an electron-transfer reaction that produces the $[Fe^{II}(CN)_5(H_2O)]^{3-}$ complex, which in turn reacts with the ligands present in the medium generating nitroprusside (see Scheme 2).

The $[Fe^{II}(CN)_5(H_2O)]^{3-}$ complex was not detected as an intermediate; in fact no intermediates were observed during the reaction. This complex is labile; the rate of water exchange was estimated to be ca. 300 s^{-1},[6] and this is consistent with the fact that the reported values of $k_{NO_2^-}$ (Scheme 2) are at least one order of magnitude faster than k_{NO}.[6,7] The rate constant k_{H^+} is also reported to be very fast under the selected conditions.[25] According to this information, the reduction by NO must be rate determining in the overall reaction (7), and $k_f = k_{NO}$. Although NO reduction of the $[Fe(CN)_5(H_2O)]^{2-}$ complex through an outer-sphere reaction is very unfavourable,[24] the possibility of an inner-sphere path can explain why the reaction is still observable.[11] Kinetic studies on the reduction of the $[Fe(CN)_5(NO_2)]^{3-}$ and $[Fe(CN)_6]^{3-}$ complexes with ascorbic acid afforded very similar activation parameters to those obtained in our study, namely $\Delta S^{\#} = -119$ J K^{-1} mol^{-1} and $\Delta V^{\#} = -10$ cm^3 mol^{-1} for the reaction of $[Fe(CN)_5(NO_2)]^{3-}$ to generate nitroprusside.[26]

Another possibility is that NO, which is in excess, reacts with the $[Fe(CN)_5(H_2O)]^{3-}$ complex (Scheme 2) to generate the $[Fe(CN)_5NO]^{3-}$ complex [reaction (4)]. The latter complex would be oxidized by the starting compound to nitroprusside, and the reaction would be autocatalytic.[11,24,27] Nevertheless, this intermediate was not detected. Moreover, experiments done in the presence of pyrazine (vide infra) showed that neutral ligands cannot compete effectively with

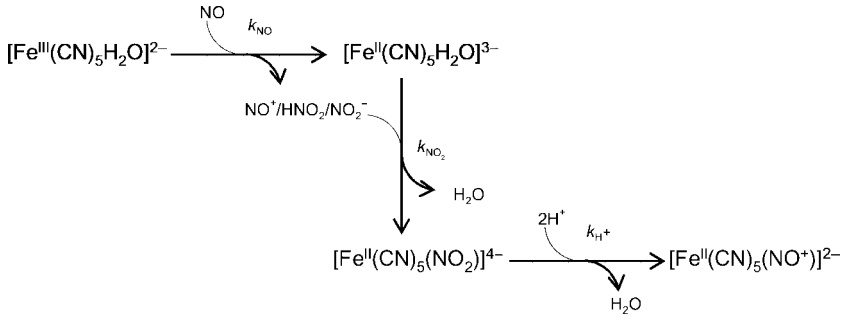

Scheme 2.

$NO^+/HNO_2/NO_2^-$ present in the second coordination sphere, since concentrations as high as 50 mM were insufficient to convert all of the reactant into the pyrazine complex.[24] On the other hand, the yield of nitroprusside for the reaction between $[Fe(CN)_5H_2O]^{3-}$ and NO at pH 3–5 was quite low: 35–45%,[11] while the reaction with the Fe^{III} complex under similar conditions generated nitroprusside quantitatively.[24] Finally, we would expect a quadratic NO concentration dependence for such an autocatalytic mechanism, according to Scheme 2 and Equation (8) (vide infra).

Reaction (7) was studied in the presence of other ligands (pyrazine and SCN^-) that could scavenge the $[Fe(CN)_5(H_2O)]^{3-}$ complex and give evidence of its presence during the reaction.[24] When SCN^- was used, a first order decay of the bands characteristic of the $[Fe(CN)_5(H_2O)]^{2-}$ complex was accompanied by formation of the $[Fe^{III}(CN)_5SCN]^{3-}$ complex, which was evidenced by its typical absorption band at 598 nm. Working at constant NO concentration, the observed rate constant depended linearly on the SCN^- concentration, with a slope of 2.3×10^{-3} M^{-1} s^{-1}. The intercept was 2.17×10^{-4} s^{-1}, which is very similar to the value obtained in the absence of SCN^-, as expected. By using pyrazine instead of SCN^-, a very similar picture was obtained, and a first-order reaction with a linear dependence on the pyrazine concentration was also observed. It is important to note that such reactions in the absence of NO are orders of magnitude slower.[22] To explain these findings, we propose the mechanism depicted in Scheme 3, where pyrazine or SCN^- compete with NO^+, HNO_2 or NO_2^- to react with the $[Fe(CN)_5(H_2O)]^{3-}$ complex. The Fe^{II} complexes thus produced are oxidized by the reactant to form the corresponding Fe^{III} compounds.

Assuming that the Fe^{II} complexes are in steady state, Equation (8) was derived.[24]

$$k_{obs} = k_{NO}[NO]\left(1 + \frac{k_L[SCN^-/pz]}{k_{NO_2^-}[HNO_2]}\right) \quad (8)$$

The rate law predicts a linear dependence of k_{obs} on the pyrazine and SCN^- concentrations, as was observed, which provides evidence for the role of the $[Fe(CN)_5(H_2O)]^{3-}$ complex as an intermediate and strong support for the proposed mechanism.

To obtain additional information in favour of this proposal, the reaction of NO with other $[Fe^{III}(CN)_5L]$ complexes was studied. When L = pyridine, the corresponding Fe^{II} complex was observed as an intermediate. Moreover, the $[Fe(CN)_5(NO_2)]^{3-}$ complex generates nitroprusside quantitatively when it reacts with NO at pH 5.[24]

The present reaction and the proposed mechanism were discussed in a recent review, and an alternative mechanism was proposed.[27] It involves the formation of a seven-coordinate intermediate between NO and the starting compound $[Fe^{II}(CN)_5(H_2O)(NO^+)]^{2-}$. This intermediate would lead to the formation of nitroprusside through the release of water or would lead to the formation of $[Fe(CN)_5(H_2O)]^{3-}$ through the release of NO^+. As we mentioned before, the Fe^{II}–NO^+ bond is very stable, and we find it rather unlikely that the $[Fe(CN)_5(H_2O)]^{3-}$ complex would be generated as an intermediate in this way. Alternatively, the formation of a related precursor between NO and the starting complex could be proposed, in which NO interacts with the

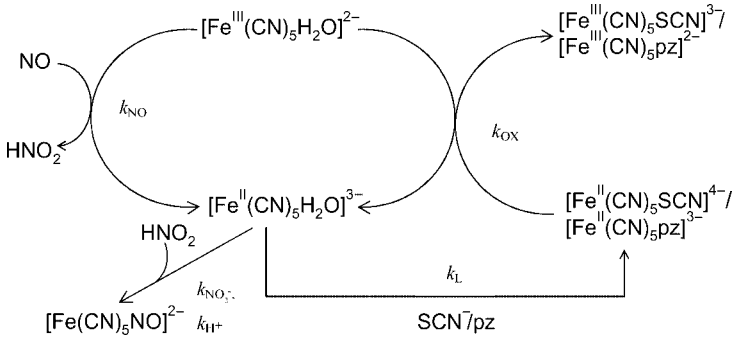

Scheme 3.

CN^- ligands without changing the first coordination sphere of the Fe centre.[11] In this way, the reaction would proceed through an inner-sphere electron-transfer reaction, generating also the $[Fe(CN)_5(H_2O)]^{3-}$ complex. This mechanism would provide an explanation why neutral ligands like pyrazine cannot effectively compete with HNO_2. This mechanism does not change our conclusions and the main argument in favour of a prior reduction of the Fe^{III} complex, in the absence of a change in the first coordination sphere, followed by coordination of HNO_2/NO_2^- and final conversion into nitroprusside.

6. Reactions of NO with Iron(III) Porphyrin Complexes

In terms of biological activity, the most significant property of NO is its interactions with iron centres of hemoproteins. It has been suggested that many heme-based enzymes have their activity modulated by NO in vivo. Under bioregulatory conditions, two important target enzymes of NO action in biological systems such as mammalian guanylate cyclase[28] and fungal nitric oxide reductase[29] utilize the iron-heme-cofactors. NO–iron-porphyrin interactions have been shown to be responsible for the inhibition of certain hemoproteins that under physiological conditions bind/or activate dioxygen, including hemoglobin, myoglobin and the cytochrome P450 super family.[30] Moreover, NO binding to the iron-heme centre of a ferriheme salivary protein (nitrophorins) is considered to play an important role in vasodilating effects of blood sucking insects.[31] Since in vivo interactions of NO with iron centres of hemoproteins affect physiological and pathophysiological actions, numerous mechanistic and structural studies on NO binding to iron hemes and their biomimetic models have been undertaken.[32] However, because of the close interplay of many factors that govern the dynamics of NO binding to iron heme centres and of NO release from heme nitrosyls (e.g. oxidation state and spin state of the iron centre, type of the heme ring, number and identity of the axial ligands, interactions of the amino acid residues around the active site in the protein pocket, protein superstructure, accessibility of the iron heme centre to the NO ligand, polarity of the reaction media, etc.), the elucidation of the details of the molecular pathways followed during NO coordination to and dissociation from iron hemes is very difficult and far from complete.

Our own contribution to the understanding of the role of these factors involves in-depth mechanistic and kinetic investigations of the reversible NO binding to selected ferriheme proteins and model iron(III) porphyrins that can supplement other results from structural, kinetic and thermodynamic studies available to date on this topic. In contrast to the NO reactions with iron(II) centres, which are inconvenient to measure because of slow NO dissociation kinetics, the kinetic behaviour of the reactions with iron(III) centres enables the determination of both association and dissociation processes of NO under physiological conditions. In this context, we present an overview of some developments in the mechanistic chemistry involving reactions of selected iron(III) porphyrin complexes [hemoproteins and synthetic iron(III) porphyrin models] with NO, which gives an opportunity to gain insight into the mechanisms of formation and decay of nitrosyl hemoproteins in vivo.

In acidic aqueous solution, NO reversibly binds to six-coordinate, water-soluble iron(III) porphyrin complexes such as $(TPPS^{4-})Fe(H_2O)_2$, $(TMPS^{4-})Fe(H_2O)_2$ and $(TMPyP^{4+})Fe(H_2O)_2$, where TPPS = tetraphenylporphyrinato-4-sulfonate, TMPS = tetramesitylporphyrinato-4-sulfonate and TMPyP = tetra(4-*N*-methylpyridyl)porphyrin.[33,34] Coordination of NO to these hemoproteins induces a low-spin electronic configuration of the metal centre in the resulting nitrosyl derivative.[35] According to the Enemark and Feltham formalism,[1] the nitrosyl products of NO binding to iron(III) porphyrins are typically diamagnetic complexes (type $\{Fe–NO\}^6$) with a linear $Fe^{II}–NO^+$ unit, as has been demonstrated by ^{15}N NMR and IR spectroscopy.[36,37] In general, the kinetic behaviour of NO binding to the above-mentioned iron(III) porphyrins is described by the relatively high values for the association and dissociation rate constants (Table 3). The "on" rates for NO binding to these complexes are, however, about three orders of magnitude lower than those found for the iron(II) analogues.[33] In addition, the $(TMPyP^{4+})Fe(H_2O)_2$ complex with a 4+ charge on the porphyrin ring reacts with nitric oxide 25–100 slower than the other two systems, $\{(TPPS^{4-})Fe(H_2O)_2$ and $(TMPS^{4-})Fe(H_2O)_2\}$, in which the porphyrin carries a 4– charge. A close examination of the activation parameters, especially the activation volumes, determined for these reactions appears to be very helpful in understanding the kinetic trends observed in NO binding reactions for the studied iron(III) porphyrins.

The reactions of NO binding to $(TPPS^{4-})Fe(H_2O)_2$ and $(TMPS^{4-})Fe(H_2O)_2$ are described by large and positive values for the activation entropy and activation volume for both the "on" and "off" processes (Table 3), which are signatures for ligand substitution dominated by dissociation of a water molecule as depicted in Scheme 4 ("D" mechanism).[33]

Thus, in acidic medium the dynamics of the reversible binding of NO to the iron(III) centres of $(TPPS^{4-})Fe(H_2O)_2$ and $(TMPS^{4-})Fe(H_2O)_2$ seems to be mainly controlled by the lability of the metal centre. An analogous dissociatively activated mechanism was also proposed for NO release from the nitrosyl complexes of these iron(III) porphyrins. A dissociative mechanism requires that the exchange of the water molecule proceeds in a comparable way. Indeed, variable temperature/pressure NMR studies on the water-exchange kinetics of these iron(III) porphyrin diaqua species[38] very nicely confirmed that activation parameters found for the nitrosylation reaction of these two complexes are largely defined by a dissociative mechanism and the limiting step is the dissociation of the coordinated water molecule. On the basis of this mechanism, it can be explained why NO association reactions with iron(II) porphyrins are

Table 3. Rate constants and activation parameters for reversible binding of NO to water-soluble iron(III) porphyrins.

Complex	k_{on} [$M^{-1}s^{-1}$][a] k_{off} [s^{-1}][a]	$\Delta H^{\#}$ [$kJ\,mol^{-1}$]	$\Delta S^{\#}$ [$J\,K^{-1}\,mol^{-1}$]	$\Delta V^{\#}$ [$cm^3\,mol^{-1}$]	Proposed mechanism	Ref.
$(TPPS^{4-})Fe(H_2O)_2$	4.5×10^5	69 ± 3	95 ± 10	9 ± 1	D	[33]
Int[a] = 20%	500 ± 400	76 ± 6	60 ± 11	18 ± 2	D	
$(TMPS^{4-})Fe(H_2O)_2$	2.8×10^6	57 ± 3	69 ± 11	13 ± 1	D	[33]
Int[a] = 26%	900 ± 200	84 ± 3	94 ± 10	17 ± 3	D	
$(TMPS^{4-})Fe(OH)$	1.3×10^4[b]	28 ± 1	-71 ± 2	-16 ± 0.4	A	[43]
	7.0 ± 0.1[b]	90 ± 1	76 ± 3	7.4 ± 1		
$(TMPyP^{4+})Fe(H_2O)_2$	2.9×10^4	67 ± 4	67 ± 13	3.9 ± 1	I_d	[34]
Int[a] = 7%	59 ± 4	113 ± 5	169 ± 18	17 ± 0.2	D	
$(P^{8+})Fe(H_2O)_2$	1.5×10^4	77 ± 3	94 ± 12	1.5 ± 0.3	I_d or I	[41]
Int[a] = 10%	26 ± 0.5	83 ± 4	61 ± 14	9.3 ± 0.5	I_d	
$(P^{8+})Fe(OH)(H_2O)$	1.6×10^3	41 ± 1	-45 ± 2	-13.8 ± 0.4	A	[41]
	6.2 ± 0.1	72 ± 2	12 ± 5	2.6 ± 0.2		
$(P^{8-})Fe(H_2O)_2$	8.2×10^5	51 ± 0.5	40 ± 2	6.1 ± 0.1	I_d or D	[40]
Int[a] = 24%	220 ± 2	107 ± 3	160 ± 10	16.8 ± 0.4	D	
$(P^{8-})Fe(OH)$	5.1×10^4	35 ± 0.4	-39 ± 1	-6.1 ± 0.2	A	[40]
	11 ± 0.3	107 ± 2	136 ± 7	17 ± 3		
metMb	4.8×10^4	71 ± 2	82 ± 7	21 ± 1	D	[45]
	29 ± 1.5	78 ± 2	46 ± 7	16 ± 1	D	

[a] Contribution of the intermediate-spin state (S = 3/2) in the corresponding spin-admixed iron(III) diaqua porphyrin complex. [b] Determined at 22 °C.

$$Fe^{III}(Por)(H_2O)_2 \underset{k_{-1}}{\overset{k_1}{\rightleftharpoons}} Fe^{III}(Por)(H_2O) + H_2O$$

$$Fe^{III}(Por)(H_2O) + NO \underset{k_{-2}}{\overset{k_2}{\rightleftharpoons}} Fe^{III}(Por)(H_2O)(NO)$$

Scheme 4.

several orders of magnitude faster than those with the iron(III) analogues. Since high-spin iron(II) porphyrins may be five-coordinate, NO binding to the metal centre can proceed without first displacing another ligand [for example a water molecule in the iron(III) porphyrin diaqua species]. Another important conclusion that can be drawn from these studies is that the free radical nature of NO appears to have only a minor (if any) influence on the NO substitution dynamics at the metal centres of iron(III) porphyrins, thus NO behaves as a typical Lewis base donor.

Another mechanistic scenario was observed for the NO interaction with the positively charged $(TMPyP^{4+})Fe(H_2O)_2$.[34] The much slower bond cleavage observed for this system [both NO association and dissociation rate constants are significantly lower than those for the iron(III) porphyrins carrying a 4– charge] must be closely related to the electrophilicity of the iron centre in the TMPyP complex. From the activation parameters found for this system (Table 3), it is clear that in this case the substitution of a coordinated water molecule by NO follows a dissociative interchange (I_d) mechanism. The changeover from a limiting dissociative substitution mechanism observed for the corresponding iron(III) TPPS and -TMPS complexes to an I_d mechanism found in this case can be ascribed to the lower lability of the coordinated water molecule in the $(TMPyP^{4+})Fe(H_2O)_2$ complex. This finding appears to be in line with the trend observed for the rate constants and activation parameters measured for water-exchange reactions of these three complexes,[38] where the water-exchange reaction at the iron(III) centre of the positively charged porphyrin is much slower than for the other studied systems with a 4– charge on the porphyrin rings. It seems that in acidic medium, water-exchange processes control the rate and mechanism of the nitrosylation reactions of all three diaqua iron(III) porphyrins in which the labilization of the $Fe–OH_2$ bond is determined by the electron-donating/withdrawing properties of the substituted porphyrin, which in turn depend on the anionic/cationic nature of the substituents, respectively.

In order to better understand the influence of the porphyrin microenvironment in iron(III) porphyrin systems on the rate and mechanism of NO binding and release, as well as to establish the relationship between the structure of the prosthetic group and its reactivity toward NO in various hemoproteins in vivo, two new iron(III) porphyrin models, a highly negatively charged {$(P^{8-})Fe^{III}$ = [5⁴,10⁴,15⁴,20⁴-tetra-*tert*-butyl-5²,5⁶,15²,15⁶-tetrakis(2,2-biscarboxylatoethyl)-5,10,15,20-tetraphenylporphyrin]iron(III)} and a highly positively charged {$(P^{8+})Fe^{III}$ = [5,10,15,20-tetrakis(4′-*tert*-butyl-2′,6′-bis(4-*tert*-butylpyridine)phenyl)porphyrinato]iron(III)} water-soluble porphyrin, have been synthesized[39,40] (see Figure 6). A detailed kinetic and mechanistic description of the reversible binding of NO to these complexes in aqueous solution at low and high pH has been presented recently.[40,41]

In general, iron(III) porphyrins may occur as five- and six-coordinate complexes in which the iron atom can exist in three different spin states, the low-spin state (S = 1/2, typically six-coordinate with short axial and equatorial bonds), high-spin state (S = 5/2, often five-coordinate with elongated equatorial bonds and displacement of the iron atom out of the porphyrin plane) and intermediate-spin state (S = 3/2 with short equatorial and elongated axial bonds). In addition, depending on the nature of the axial ligands and porphyrin-ring substituents, the spin state of

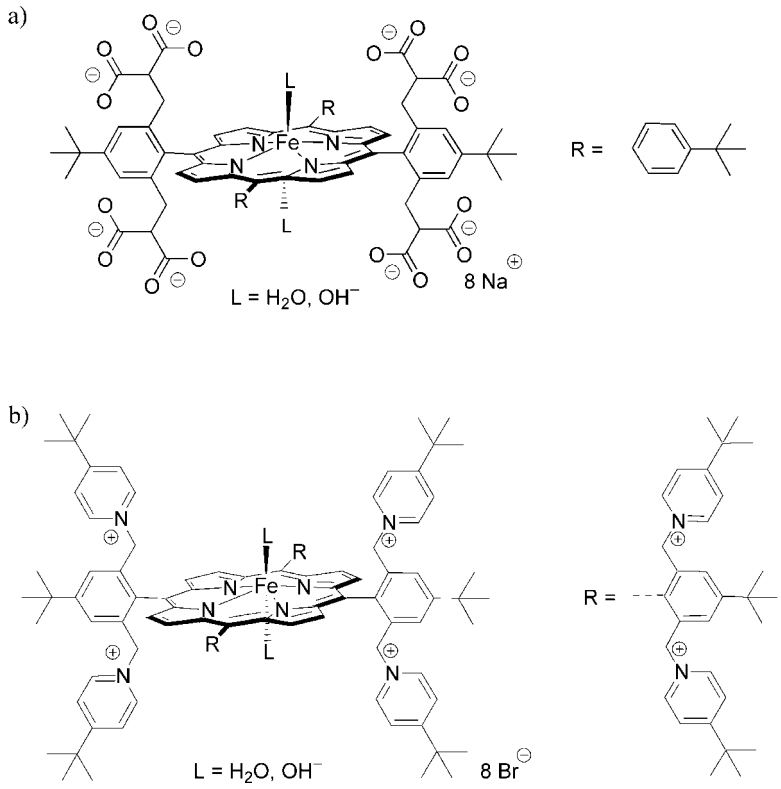

Figure 6. Structures of (a) a highly negatively charged $(P^{8-})Fe^{III}(L)_2$[40] and (b) a highly positively charged $(P^{8+})Fe^{III}(L)_2$[39] iron(III) porphyrin model.

the iron(III) in many iron(III) porphyrins can be described as admixed intermediate, in which varying ratios of $S = 5/2$ and $S = 3/2$ admixing were noted.[42] In this context, it was revealed that introduction of four flexible malonate substituents on the highly negatively charged porphyrin $(P^{8-})Fe^{III}(H_2O)_2$ (in buffered, aqueous solution at pH = 7) leads to significant electronic effects on the iron(III) centre, which are reflected by the relatively high contribution of the $S = 3/2$ spin state in the spin-admixed intermediate.[40] Moreover, these electronic effects together with the possible through-space interactions of negatively charged substituents with coordinated water resulted in an increase in the pK_a value of the coordinated H_2O to the highest value reported to date. With regard to the kinetic behaviour of $(P^{8-})Fe^{III}(H_2O)_2$ in its reaction with NO, a relatively high contribution of the $S = 3/2$ spin state in the spin-admixed state of this complex in comparison with those of other iron(III) porphyrins correlates very well with high NO coordination rates (see Table 3) and the high lability of coordinated water measured for this system.[40] A comparison of the rate and activation parameters for the binding and release of NO for $(P^{8-})Fe^{III}(H_2O)_2$ in aqueous solution at pH = 7 (Table 3) with those reported for other diaqua-ligated iron(III) porphyrin species leads to the conclusion that the reactivity of this complex toward NO is described by the same dissociative (D or I_d) mechanism, in which the NO association reaction is controlled by substitution of a water molecule. Similarly, the release of NO from the corresponding nitrosyl complex also follows a dissociative mechanism.

Markedly smaller (in absolute values) NO association and dissociation rate constants as well as activation parameters (especially activation volumes) were obtained for a highly positively charged water-soluble porphyrin, viz. $(P^{8+})Fe^{III}(H_2O)_2$ (Table 3) in which the Fe^{III} centre is weakly spin-admixed with only a 10-% contribution of the intermediate $S = 3/2$ spin state.[41] NO coordination to the iron(III) centre of this highly positively charged porphyrin appears to follow an I_d or even I mechanism (without a predominant a- or d-character). In a similar way, the substantially smaller value of the activation volume determined for NO release from the nitrosyl complex of $(P^{8+})Fe^{III}(H_2O)_2$ than the corresponding values reported for other porphyrin nitrosyls clearly implies a less dissociative mode for NO dissociation from the highly positively charged iron(III) porphyrin.

In summary, the results from the kinetic and mechanistic studies presented above for reversible NO binding to the water-soluble iron(III) diaqua-ligated porphyrins (Table 3) clearly demonstrate that the identity and charge of the substituents in the porphyrin periphery strongly affect the dynamics of both the binding and release of NO. These effects can be summarized as follows: (i) Electron-donating *meso* substituents on the porphyrin rings increase and electron-withdrawing groups decrease electron density on the iron(III) centres, which is reflected by an increase or a decrease in the contribution of the $S = 3/2$ spin state in the spin-admixed system, respectively. (ii) Electron density on the iron(III) centre influences the lability of the coordinated

water molecule. Thus, a porphyrin-induced increase in electron density on the iron(III) centre facilitates breakage of the Fe–H_2O bond, whereas for porphyrins with electron-withdrawing *meso* substituents, this bond is more stabilized. (iii) As a result of (i) and (ii), the rate of NO binding to iron(III) diaqua-ligated porphyrins increases with increasing electron donation from the porphyrin *meso* substituents, which is also reflected by the change in the mechanism of NO coordination to the iron(III) centre from predominantly dissociative for the porphyrins with electron-donating *meso* substituents to interchange (I_d or I) for the systems carrying electron-withdrawing *meso* substituents on the porphyrin rings. (iv) Electron-donating groups on the porphyrin rings destabilize, whereas electron-withdrawing substituents stabilize, the Fe^{II}–NO^+ bond in the nitrosyl complexes of (P)Fe(H_2O)$_2$, which is illustrated by the variation in k_{off} for the complexes studied. In general, NO dissociation from nitrosyl porphyrins is interpreted in terms of a dissociative mechanism. However, a decrease in the electron-donation from the porphyrin substituents was shown to result in a less dissociative mode for NO release from the corresponding nitrosyl complex.

The reactivity pattern presented above for the iron(III) diaqua-ligated porphyrins points to a crucial role of the lability of the coordinated water molecule in the dynamics of the reversible binding of NO to model iron(III) porphyrins. However, our recent systematic studies on the reactivity of various water-soluble (P)Fe^{III} species towards NO revealed that interactions of NO with heme centres need not always be controlled by the lability/accessibility of the metal centre, but can be determined by electronic and structural factors such as reorganization of the spin density of the iron centre and the accompanying structural changes.[40,41,43]

It has been demonstrated that the rate and mechanism of nitrosylation of water-soluble iron(III) porphyrin complexes can be nicely tuned by the pH of the solution, which determines the nature and number of the axial ligands on the (P)Fe^{III} species and thereby controls the coordination number, spin state and reactivity of the iron(III) centre toward NO.[43] In this context, kinetic and mechanistic investigations on the reactions of NO with monohydroxo-ligated forms of (P)Fe^{III} [formed by deprotonation of coordinated water in (P)Fe(H_2O)$_2$ at pH > pK_a] were performed for the first time.[40,41,43] In general, according to the known *trans*-labilizing effect of the hydroxo ligand, it can be expected that the presence of a more labile water molecule in the position *trans* to OH^- [or even its absence as revealed for example in the ($TMPS^{4-}$)Fe^{III} and (P^{8-})Fe^{III} species, which exist as five-coordinate monohydroxo complexes at high pH] should result in a significant increase in the NO binding rate constants relative to those measured for the corresponding iron(III) diaqua-ligated species. Surprisingly, NO rate constants and activation parameters determined for the monohydroxo forms of (P)Fe^{III} appear to be significantly smaller than those found for the (P)Fe(H_2O)$_2$ species, indicating that NO coordination to these complexes is no longer controlled by the lability or accessibility of the iron(III) centre. Obviously, this must involve a changeover

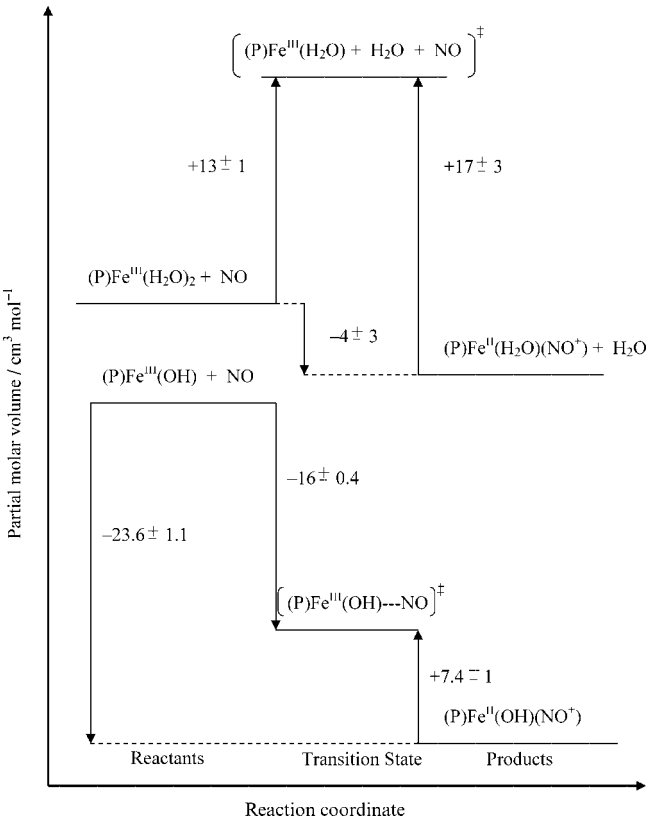

Figure 7. Volume profiles for reversible NO binding to ($TMPS^{4-}$)-$Fe^{III}(H_2O)_2$[33c] (top) and ($TMPS^{4-}$)Fe^{III}(OH) (bottom).[43]

in the mechanism of NO binding from dissociative in iron(III) diaqua-ligated species to associatively activated in the (P)Fe^{III}(OH) forms. This mechanistic difference can be nicely illustrated by a comparison of the volume profiles constructed for the reactions of reversible binding of NO to ($TMPS^{4-}$)$Fe^{III}(H_2O)_2$ and ($TMPS^{4-}$)Fe^{III}(OH), as depicted in Figure 7.

The associatively activated mechanism proposed for NO coordination to ($TMPS^{4-}$)Fe^{III}(OH) involves the diffusion-controlled formation of an encounter complex, {(P)-Fe^{III}(OH)‖NO}, and subsequent rate-determining Fe^{II}–NO^+ bond formation. A similar mechanism was proposed previously for NO binding to the high-spin iron(II) porphyrins[32b,33c] and to substrate-bound cytochrome P450.[44] The significantly slower (and therefore rate-limiting) Fe^{II}–NO^+ bond formation during NO coordination to monohydroxo iron(III) porphyrins than those observed for the nitrosylation reactions of (P)Fe(H_2O)$_2$ species (in this case Fe^{II}–NO^+ bond formation is fast and a less energetically demanding process) can be ascribed to the difference in the spin reorganization of the iron(III) centre upon NO binding at low and high pH. Accordingly, the overall spin-state change accompanying the formation of low-spin ($TMPS^{4-}$)-$Fe^{II}(NO^+)$ from purely high-spin ($TMPS^{4-}$)Fe^{III}(OH) (S = 5/2 → S = 0) is larger than that occurring upon binding of NO to the spin-admixed, diaqua-ligated complex (S = 5/2, 3/2 → S = 0). This marked difference in the spin reorganiza-

tion and the accompanying structural changes [in the purely high-spin $(TMPS^{4-})Fe^{III}(OH)$, the iron atom is displaced out of the porphyrin plane] can be responsible for the observed ca. 100-fold decrease in the NO rate constants at high pH and for the changeover in the mechanism of NO coordination to the complexes studied.

In addition to the effects associated with the lability/accessibility of the metal centre, the spin reorganization of the iron atom and the structural changes that were discussed above in detail, a number of other factors resulting from the presence of the protein coat, such as hydrogen-bonding interactions of the amino acid residues around the active site, polarity of the protein pocket, accessibility of the heme prosthetic group to the solvent, etc., should be considered in the interpretation of reactivity patterns observed for the reversible binding of NO to iron(III) centres of hemoproteins. Indeed, the results from mechanistic studies on the interactions of NO with native ferriheme proteins and comparison to those obtained for "free" iron(III) model porphyrins revealed the important role of the heme pocket in NO interactions with hemoproteins.[45,46] This can be illustrated by mechanistic studies on the reversible binding to metmyoglobin (metMb).[45] Like the iron(III) models $[(TPPS^{4-})Fe^{III}(H_2O)_2$ and $(TMPS^{4-})Fe^{III}(H_2O)_2]$, the iron(III) centre of metmyoglobin is six-coordinate and a water molecule occupies the site at which NO will coordinate. Activation parameters found for NO interaction with metMb (Table 3) clearly evidence the similar mechanistic behaviour of metmyoglobin and model iron(III) porphyrins at low pH, i.e. NO coordination to the iron(III) centre follows a dissociative mechanism controlled by the lability of the water molecule. However, close inspection of the activation volumes determined for these systems indicate that the value of $\Delta V^{\#}_{on}$ observed for the binding of NO to metMb is significantly larger than the corresponding values observed for "free" iron(III) porphyrins (see Figure 8) and therefore cannot reflect only the volume changes associated with dissociation of the water molecule from an octahedral complex (≈13 $cm^3 mol^{-1}$[47]) as was thought for the model complexes. This finding suggests that the protein may undergo some structural rearrangement upon release of coordinated water prior to the binding of NO, which can lead to a further increase in the size of the protein pocket in the transition state. This conclusion was confirmed by the results from XAFS structural studies on nitrosylated metMb.[48] The importance of the protein pocket in the interaction of NO with metmyoglobin can also be demonstrated by a comparison of the NO dissociation rate constants observed for the nitrosyl complexes of metMb and iron(III) porphyrin models $(TPPS^{4-})Fe^{III}(H_2O)_2$ and $(TMPS^{4-})Fe^{III}(H_2O)_2$ (Table 3). The much lower values of k_{off} reported for the metMb/NO system than the corresponding values observed for porphyrin models can be interpreted in terms of the stabilization of the Fe^{II}–NO^+ moiety by hydrogen-bonding interactions with the residues of the amino acids in the protein pocket. Obviously, the NO molecule cannot be as effectively "caged" after coordination to the iron(III) centres of "free" porphyrin models.

The essential contribution of the protein architecture in the dynamics of reversible NO binding to heme proteins has also been revealed by flash photolysis studies of the analogous nitrosyl complex of ferrous myoglobin (Mb).[49] The existence of multiple geminate-type intermediates in the recombination pathway of Mb(NO) has been ascribed to the presence of the protein pocket from which NO released after the laser flash cannot escape significantly from the protein as recombination occurs much faster than dissociation of the {Mb, NO} geminate pair.

Another important example of protein influence on the kinetics of NO binding to heme centres in hemoproteins can be illustrated by the reaction of NO with ferric and ferrous cytochrome *c* (Cyt *c*) in which the protein limits access of NO molecules to the iron centre.[33a,50] Since the axial ligands in Cyt *c* are occupied by histidine and methionine residues in both oxidation states of the iron centre, coordination of NO must involve displacement of a relatively tightly bound axial ligand (methionine or histidine). As a result, NO binding rate constants observed for Cyt c^{II}

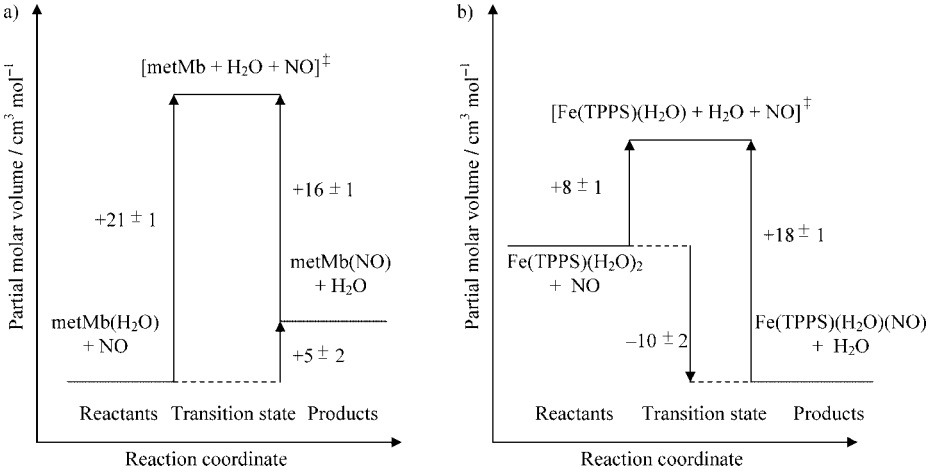

Figure 8. Comparison of the volume profiles constructed for the reversible binding of NO to (a) metmyoglobin[45] and (b) water-soluble $Fe^{III}(TPPS)(H_2O)_2$.[33]

and Cyt c^{III} are unusually small relative to rate constants obtained for ferric and ferrous hemoproteins in which access to the metal centre for the entering NO ligand is not limited by the protein (or the coordination site is occupied by a very labile ligand such as a water molecule in metMb).

7. Reactions of NO with $P450_{cam}$ and Model Complexes

Since the nature of the anionic proximal ligand coordinated to the iron(III) centre plays a crucial role in controlling the properties and reactivity of hemoproteins in numerous catalytic processes,[51] the super-family of cytochromes P450 with its quite unusual thiolate ligation attracts particular attention with regard to the spin-state equilibria of the resting state, the redox potential of the iron(III) porphyrin and the electronic nature of the high-valent iron(IV) oxo species. In order to elucidate the mechanism of action of cytochrome P450 in vivo and to understand the essence of its biological function, it is very important to gain detailed mechanistic insight into binding of small molecules such as O_2, NO and CO to the catalytic site of this enzyme. Unlike carbon monoxide and dioxygen, NO can bind to both oxidation states of cytochrome P450; the nitrosyl complexes of the ferrous forms with their electronic structure and geometry resemble the physiologically important dioxygen complexes of P450 enzymes. Furthermore, several pieces of evidence revealed that cytochromes P450 might be primary targets for NO action in vivo.[52] Since the reactions of ferrous cytochromes P450 with small molecules have already been extensively investigated, we have focused our attention on the kinetics and mechanistic interpretation of the reversible binding of NO to ferric cytochrome $P450_{cam}$ (isolated from bacterium *Pseudomonas putida*) in the absence and presence of the substrate (1*R*-camphor).[44] The substrate-free ferric $P450_{cam}$ is a low-spin (S = 1/2), six-coordinate complex with a water cluster bound at the distal site *trans* to the cysteine axial ligand in the proximal position. Upon binding of camphor to the active site, water molecules are expelled from the coordination sphere, which leads to the formation of a high-spin (S = 5/2), five-coordinate iron-heme centre. Coordination of NO to the substrate-free or camphor-bound form of $P450_{cam}$ results in the formation of the relatively stable, six-coordinate nitrosyl complex. Earlier EPR[53] and resonance Raman[54] studies on the NO adduct of $P450_{cam}$ showed that the nitrosyl complex of $P450_{cam}$ is a low-spin complex (EPR silent) in which the Fe–NO group adopts a linear structure in the absence of substrate, but becomes slightly bent upon binding of camphor. However, subsequent crystallographic characterization of the Fe–N–O linkage in the $\{FeNO\}^6$ species (models and enzymes)[55] revealed that such systems can also display an axial NO bending feature coupled with tilting of the Fe–NO group. The tilting/bending mode of the axial NO ligand in nitrosyl complexes of iron(III) porphyrins was found to be intrinsic to species of the type $(Por)Fe^{III}(NO)X$, where X is a strong σ-donor ligand.[55a]

Binding of NO to the substrate-free $P450_{cam}$ was shown to exhibit biphasic kinetics, which can be interpreted in terms of an equilibrium between conformational substates in cytochrome P450 (which is the effect of different hydrogen-bonding networks between differently packed water molecules in the heme pocket).[44] The NO binding rate constants and activation parameters determined for both reaction steps (Table 4) are consistent with the operation of a limiting dissociative ligand-substitution mechanism, in which the lability of coordinated water dominates the reactivity of the iron(III) centre with NO.

It should be noted that a similar mechanism was proposed for NO binding to metMb and synthetic water-soluble $(P)Fe^{III}(H_2O)_2$ complexes. In agreement with the principle of microscopic reversibility, the activation parameters found for the release of NO from the nitrosyl complex of substrate-free $P450_{cam}$ also indicate a rate-limiting dissociative mechanism. The overall reaction volume determined for this system is close to zero and is very similar to that found for NO binding to metmyoglobin. The apparent larger value for $\Delta V^{\#}_{on}$ (which represents volume changes associated with a pathway in which a water molecule is dissociated) reported for the reaction between NO and substrate-free $P450_{cam}$ relative to that found for the metMb/NO system can be accounted for in terms of much higher structural rearrangement in the protein pocket of $P450_{cam}$ during dissociation of the water molecule that is additionally bound to the ordered water cluster. Formation of the five-coordinate transition-state Fe^{III} complex is associated with a change in spin state from low-spin to high-spin, which is accompanied by a volume increase of between 12 and 15 $cm^3 mol^{-1}$ on the basis of literature data for such spin-state changes.

A different mechanistic scenario was observed for the reversible binding of NO to the camphor-bound form of cytochrome $P450_{cam}$.[44] As already mentioned, the substrate-bound $P450_{cam}$ is a five-coordinate, high-spin complex with no water molecule occupying the sixth coordination position of the iron(III) centre. The NO association rate constants determined for this complex appear to be significantly higher than those reported for the substrate-free $P450_{cam}$ (Table 4). Moreover, the presence of camphor markedly affects not only the NO binding rate constants but also NO release from the corresponding nitrosyl complex. The substantial negative values for the activation entropy and activation volume found for the "on" reaction (Table 4) clearly indicate that the mechanistic pathways for NO coordination to the iron(III) centres of the substrate-free and camphor-bound form of $P450_{cam}$ are completely different. Since the Fe^{III}-heme centre in substrate-bound $P450_{cam}$ is five-coordinate, formation of an Fe–NO bond does not require initial displacement of a water molecule, and therefore the ligation cannot be limited by the rate of H_2O dissociation as was observed for the reaction with substrate-free $P450_{cam}$. These features are consistent with the associatively activated mechanism in which an encounter complex, $\{(P)Fe^{III}\|NO\}$, is formed prior to NO bond formation, as was also proposed for the reaction of NO with

Table 4. Comparison of the rate and equilibrium constants, and thermodynamic and kinetic parameters for NO binding to the iron(III) centre in $P450_{cam}$ (in the absence and presence of camphor)[17] and model complexes.

	$P450_{cam}$ resting state[44]	$P450_{cam}$ + camphor ($E{\cdot}S\text{-}P450_{cam}$)[44]	SR complex in methanol[62]	Complex **3** in toluene[67]	Complex **4** in methanol[67]
k_{on} [$M^{-1}s^{-1}$][a]	$(3.20 \pm 0.02) \times 10^5$	$(3.2 \pm 0.5) \times 10^6$	$(2.7 \pm 0.2) \times 10^6$	$(1.80 \pm 0.05) \times 10^6$	$(0.6 \pm 0.05) \times 10^5$
$\Delta H^{\#}_{on}$ [kJ mol^{-1}]	92 ± 1	$14. 1 \pm 0.1$	75 ± 3	4 ± 2	14 ± 1
$\Delta S^{\#}_{on}$ [J mol^{-1} K^{-1}]	$+169 \pm 4$	-73.1 ± 0.4	$+130 \pm 11$	-111 ± 6	-107 ± 3
$\Delta G^{\#}_{on}$ [kJ mol^{-1}][a]	42 ± 1	35.9 ± 0.1	36 ± 3	37 ± 2	46 ± 1
$\Delta V^{\#}_{on}$ [cm^3 mol^{-1}]	$+28 \pm 2$	-7.3 ± 0.2	$+6.4 \pm 1$	-25 ± 1	-21 ± 4
k_{off} [s^{-1}][a]	0.35 ± 0.02	1.93 ± 0.02	1.8 ± 2.1	12470 ± 120	2249 ± 167
$\Delta H^{\#}_{off}$ [kJ mol^{-1}]	122 ± 4	83.8 ± 0.7		58 ± 1	44 ± 5
$\Delta S^{\#}_{off}$ [J mol^{-1} K^{-1}]	$+155 \pm 15$	$+41 \pm 2$		$+29 \pm 5$	-34 ± 22
$\Delta G^{\#}_{off}$ [kJ mol^{-1}][a]	76 ± 4	71.6 ± 0.7		50 ± 1	54 ± 5
$\Delta V^{\#}_{off}$ [cm^3 mol^{-1}]	$+31 \pm 1$	$+24 \pm 1$		$+7 \pm 3$	$+7 \pm 3$
K_{NO} [M^{-1}][a]	$(9.0 \pm 0.2) \times 10^5$	$(1.2 \pm 0.4) \times 10^6$		122 ± 10	26.9 ± 2.9
$\Delta H°$ [kJ mol^{-1}]	-30 ± 5	-69.7 ± 0.8		-71 ± 3	-59 ± 4
$\Delta S°$ [J mol^{-1} K^{-1}]	$+14 \pm 19$	-114 ± 2		-197 ± 10	-169 ± 13
$\Delta G°$ [kJ mol^{-1}][a]	-34 ± 4	-35.7 ± 0.7		-12 ± 3	-9 ± 4
$\Delta V°$ [cm^3 mol^{-1}]	$+3 \pm 3$	-31.3 ± 1.2		-39 ± 2	-28 ± 1

[a] At 25 °C.

ferroheme proteins[56] and their model complexes[32b,33c] or with the water-soluble monohydroxo iron(III) porphyrin models.[40,41,43] The value of the second-order rate constant for the binding of NO to camphor-bound $P450_{cam}$ is relatively small relative to the rate constants known for the diffusion-controlled reactions in water. This observation, along with the negative activation entropy and activation volume values, supports an activation-controlled reaction mechanism in which Fe–NO bond formation is the rate-determining step. In such a case, Fe–NO bond formation and the concomitant change in spin-state from high- (S = 5/2) to low spin (S = 0) should result in negative contributions to the activation entropy and activation volume. Notably, the large and positive values for the activation parameters found for the release of NO from the nitrosyl complex of camphor-bound $P450_{cam}$ are consistent with a reaction mechanism in which the iron–nitrosyl bond is broken. This process should formally involve charge transfer from iron(II) to the nitrosyl ligand (i.e. formal oxidation of Fe^{II} to Fe^{III}) with concomitant solvational changes as a result of charge distribution. The difference in the mechanistic mode observed during NO coordination to the iron(III) centre of $P450_{cam}$ in the absence and presence of substrate can be illustrated nicely by comparison of volume profiles constructed on the basis of kinetic data determined for both reactions (see Figure 9a and Figure 10a). The importance of NO bond-formation/bond-breakage processes coupled to changes in the spin state of the iron(III) centre in camphor-bound $P450_{cam}$ is reflected by a drastic volume decrease on going from the reactant to the product states, whereas the overall reaction volume measured for the nitrosylation reaction of substrate-free $P450_{cam}$ is close to zero, indicating no overall spin-state change occurs during NO binding to the low-spin, six-coordinate $P450_{cam}$. Moreover, the transition states for these reactions differ significantly in terms of the contribution arising from Fe–NO bond formation. In the case of NO binding to $P450_{cam}$ in the presence of camphor, the transition state can be described as "early", i.e. close in nature to the reactant state, which indicates that only partial bond formation accounts for this position. Subsequently, bond formation is completed and accompanied by a change in spin state.

Comparison of the NO association and dissociation rate constants obtained for the reversible binding of NO to $P450_{cam}$ with those found for other iron(III) thiolate- and imidazole-ligated proteins, led to the conclusion that it is very problematic to quantify the real *trans* effect of proximal imidazole and thiolate coordination in such systems. Taking into account that iron(III) heme proteins with even the same thiolate ligation can display quite a wide range of NO binding and release rate constants, it is clear that apart from factors arising from the coordination mode and spin state of the iron(III) centre [i.e. the lability of the leaving group (or its absence) and the identity of the axial and porphyrin ligands], other effects associated with different protein architecture of the heme active sites and their accessibility to ligands should be considered in the dynamics of reactions of NO with metal centres of biological relevance. It seems very likely that nature uses the simultaneous interplay of all these factors to achieve a desired goal, viz. regulation (facilitation or slowing down) of the rates of NO binding or release processes, depending on the physiological requirements. For example, the binding of NO to ferric $P450_{cam}$ was found to be significantly faster in the presence of camphor than in its absence. As mentioned above, this feature can be ascribed to the vacant position in the coordination sphere of the camphor-bound cytochrome. However, considering the fact that the reactions of NO with five-coordinate ferrous hemoporphyrins are about three orders of magnitude larger than those for the six-coordinate ferric analogues, the effect of the vacant distal position of iron(III) in camphor-bound $P450_{cam}$ does not seem to be so large (the NO binding rate constant is only 10 times larger in the presence of camphor than in its absence). It is likely that in this case the effect of facilitation of NO binding as a result of the free coordination site is partially compensated by other opposite effects such as the greater rigidity of the active site (binding of camphor to $P450_{cam}$ causes the pro-

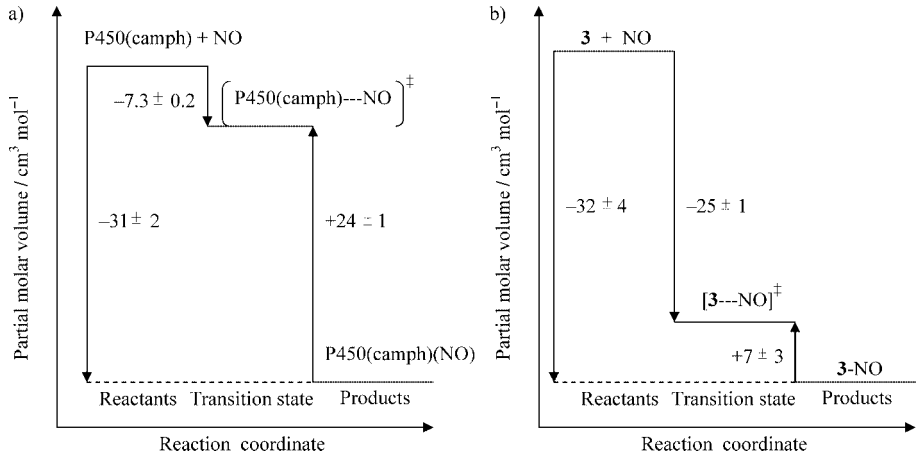

Figure 9. Comparison of volume profiles for NO binding to (a) camphor-bound $P450_{cam}$[44] and (b) complex **3** in toluene.[67]

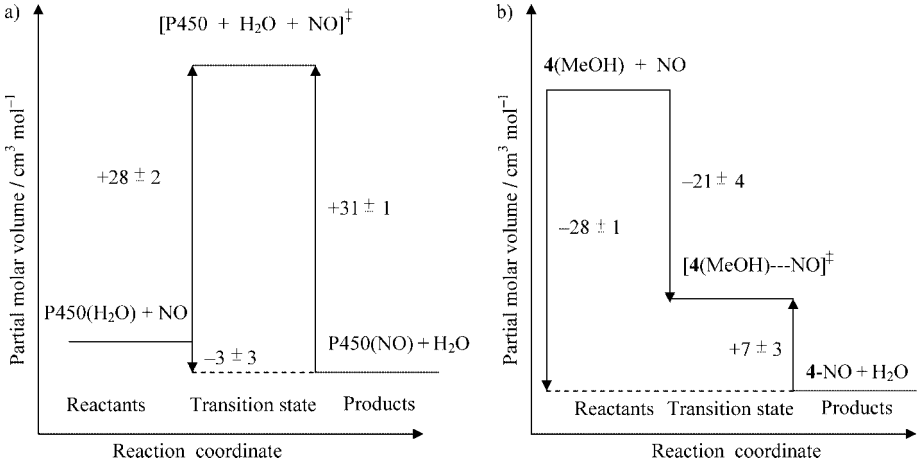

Figure 10. Volume profiles for reversible NO binding to (a) the substrate-free form of $P450_{cam}$[44] and (b) complex **4** in methanol.[67]

tein and the heme pocket to be more rigid and less compressible[57]) and/or the much larger reorganization of spin multiplicity upon NO binding to substrate-bound $P450_{cam}$ (from $S = 5/2$ to $S = 0$) than that observed for the substrate-free analogue (from $S = 1/2$ to $S = 0$).

In order to elucidate the extent to which NO binding to P450 enzymes is controlled by the metal–ligand system and the extent to which the protein heme environment can influence the dynamics of NO binding and release processes, our interest focused on mechanistic studies of NO binding to synthetic models relevant to P450 cytochrome enzymes that do not possess a protein coat. Although a number of sophisticated thiolate-ligated iron(III) porphyrins have been synthesized, most of them tend to be unstable under the employed experimental conditions, mainly because of the axial sulfur atom, which was found to be very sensitive to oxidation.[58] In this context, Higuchi and coworkers[59] prepared a stable, low-spin Fe^{III}-porphyrin alkanethiolate complex (SR complex, see complex **1** in Figure 11), in which the thiolate ligand is sterically protected by bulky pivaloyl groups. It was shown that the SR complex displays a reactivity that is similar to that of cytochrome P450 enzymes, and its bulky, protected axial thiolate ligand remains stable during the catalytic cycle.[60] Moreover, the first synthetic SR–NO complex was prepared and was characterized with the application of spectroscopic and electrochemical methods.[61] The study revealed that NO binds reversibly to the Fe^{III} centre of SR (when an equivalent amount of NO was introduced into the reaction medium), and the resulting nitrosyl complex is diamagnetic (EPR silent) with ν(N–O) and ν(Fe–N) modes that are similar to those of natural heme-thiolate-containing enzymes.

These results motivated us to investigate the mechanistic aspects of the reversible binding of NO to the SR complex in coordinating (methanol) and non-coordinating (toluene) solvents.[62] During the course of the systematic kinetic studies involving concentration-, temperature- and pressure dependences, we revealed that the interaction of the SR complex with NO cannot be described as a simple reversible binding of NO to the iron(III) centre as was reported earlier for the $P450_{cam}$/NO system.[44] Even for a low excess of NO, a rather complex reactivity pattern with several reaction steps was clearly observed. Under the conditions of low NO concentrations, NO reversibly coordinates to the SR complex in methanol with a binding rate constant that is similar to that found for the related reaction with $P450_{cam}$

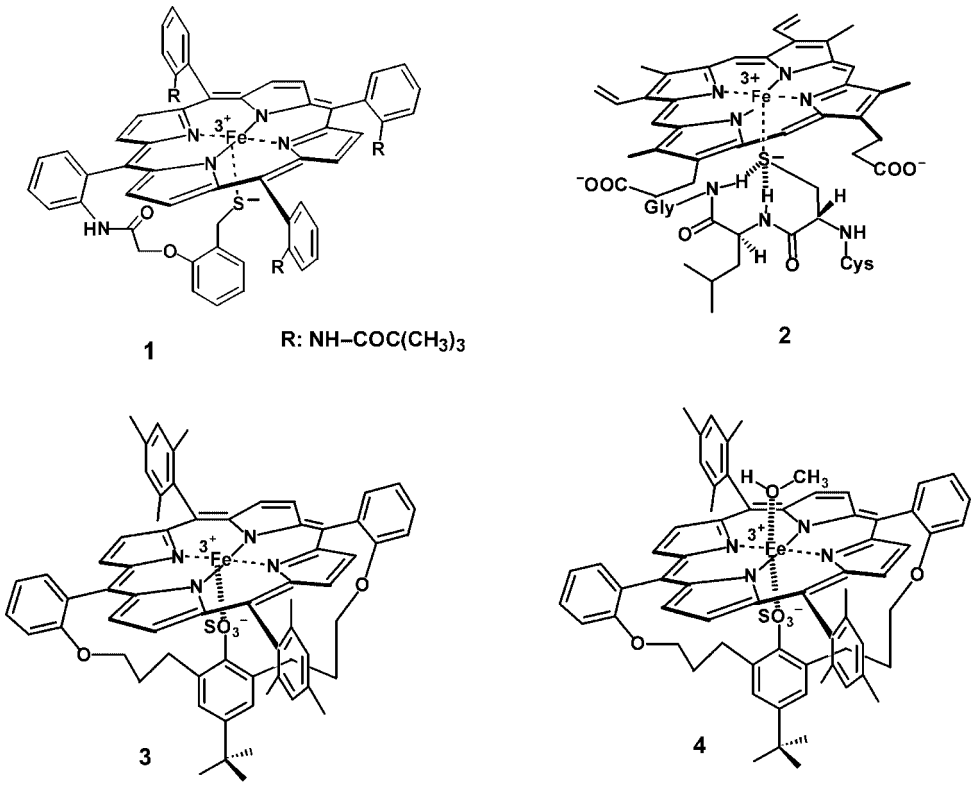

Figure 11. P450 enzyme models [**1** (SR complex),[59] **3**[65] and **4**[65]] and coordination sphere of $P450_{cam}$ (**2**).

(Table 4). The NO dissociation rate constant, although determined with a relatively large extrapolation error (because of subsequent reactions it was impossible to measure this value directly with the use of NO scavengers), is also of the same order of magnitude as that reported for the $P450_{cam}$/NO system.

The activation parameters determined for the formation of the SR–NO complex in methanol (Table 4) indicate a limiting dissociative mechanism that is dominated by dissociation of a coordinated methanol molecule. The value for the NO binding rate constant determined for this reaction in a non-coordinating solvent such as toluene is almost three orders of magnitude higher and clearly supports that the NO binding dynamics is, in this case, governed by the coordination mode of the iron(III) centre.

Under conditions of excess NO, the rapid formation of the SR–NO complex is followed by subsequent slower processes. The second observed reaction step can be accounted for in terms of direct attack of a second NO molecule at the sulfur atom of the thiolate ligand in the initially formed SR–NO complex. This leads to the formation of the five-coordinate $SR(Fe^{II})$ nitrosyl complex, which was characterized by EPR and IR spectroscopy. Although the thiolate ligand in SR is sterically protected by bulky groups, formation of the S-nitrosylated derivative under conditions of a large excess of NO does not seem unusual. It should be noted that a similar scenario was observed for the reactions between NO and the stable glutathionylcobalamin[63] and insect nitrophorins.[64] The following two slower reactions appeared to be strongly accelerated by a large excess of NO or by the presence of higher nitrogen oxides (NO_x) in the reaction medium. They can be accounted for in terms of the dynamic equilibria between higher nitrogen oxides and the reactive SR species, which results in the formation of a nitrosyl–nitrite complex of $SR(Fe^{II})$ as the final product.

In summary, although $P450_{cam}$ and the SR model display similar NO association and dissociation rate constants, their reactivity towards NO differs, leading to several NO_x-induced reaction steps in the latter case. The use of NO even in a large excess did not result in the nitrosylation of the proximal thiolate group of cytochrome $P450_{cam}$. This observation reflects very well the importance of the protein structure in the neighbourhood of the iron centre not only in controlling the coordination mode and spin state of the metal centre, but also in stabilizing thiolate coordination to the iron(III) heme centre. On the other hand, the multiple reaction steps observed for the SR/NO system can be regarded as a good model for the reactions occurring in vivo, where the dynamic equilibria involving iron(III) hemoproteins and redox-related NO_x species present under aerobic physiological conditions can lead to the rather complex reactivity pattern in which NO_x can act (i) as a ligand that coordinates to the metal centre, (ii) as a S-nitrosylation agent or (iii) as a nucleophile (catalyst), leading to the reductive nitrosylation of the iron(III) heme centres.

More suitable and inert towards oxidation and S-nitrosylation appears to be an enzyme mimic in which the thiolate group is replaced by a RSO_3^- group (complex **3**, Figure 11).[65] DFT calculations[65d] revealed that introduction of the RSO_3^- ligand significantly reduces the negative

charge localized on the oxygen atom that coordinates to the iron(III) centre. Therefore, such a system can better mimic the coordination sphere of several native P450 enzymes, in which electron donation from the sulfur atom is also reduced because of the presence of hydrogen bonding between the thiolate ligand and residues of the amino acids in the protein pocket (compare complex **2** and **3** in Figure 11). Moreover, preliminary UV/Vis[65f] and kinetic[66] experiments showed that upon treatment of complex **3** with peracid (peroxide shunt pathway), the oxoiron(IV) porphyrin π-cation radical is produced, which is regarded in the literature as a reactive intermediate responsible for the oxygen atom transfer to hydrocarbons in P450-catalyzed reactions.

To investigate the influence of the identity of the proximal and distal ligands on the dynamics of NO binding to the new synthetic model carrying the RSO_3^- group in the axial position, we performed thermodynamic and kinetic studies on NO coordination to complexes **3** (in non-coordinating toluene) and **4** (in coordinating methanol).[67] In toluene, the five-coordinate, high-spin complex **3** reminiscent of the camphor-bound $P450_{cam}$ is formed, whereas in methanol the six-coordinate complex **4** (see Figure 11) is produced, which resembles the resting state of $P450_{cam}$. As can be seen from Table 4, model complex **3**, although having no protein pocket and possessing a SO_3^- group as proximal ligand, displays a NO binding rate constant in a non-coordinating solvent that is similar to that measured for the NO association reaction of camphor-bound $P450_{cam}$. However, the rate constants for the NO release from the nitrosyl complexes of **3** and camphor-bound $P450_{cam}$ differ by almost four orders of magnitude; **3** has a significantly lower value for the NO binding constant at room temperature. However, the binding constant increases significantly as the temperature decreases. Activation parameters found for NO binding to complex **3** and to native camphor-bound $P450_{cam}$ support the same mechanism for both reactions; the mechanism is dominated by Fe^{III}–NO bond formation accompanied by a change in the iron(III) spin state (from $S = 5/2$ to $S = 0$). However, despite the similarity in the reaction volume and entropy, the volume profiles for NO binding to these complexes (Figure 9) differ substantially in terms of the position of the transition state, which can reflect different contributions arising from bond formation and change in spin state. In contrast to the volume profile constructed for the reaction between NO and camphor-bound $P450_{cam}$, reversible binding of NO to **3** is described by a "late" transition state for the association reaction and an "early" transition state for the dissociation reaction. This feature is in agreement with relatively slow "on" and fast "off" reactions and results in the much lower binding constant for NO coordination to **3** than to the native $P450_{cam}$.

When the reaction between NO and the model complex **3** was carried out in a coordinating solvent (methanol), a different mechanistic scenario was observed, indicating the importance of the spin state and the coordination mode of the iron(III) centre in the NO binding process.[67] In methanol, complex **4** is a six-coordinate, high-spin species. The presence of methanol coordinated to iron(III) slows down the binding of NO to **4** by about a factor of 10 relative to the binding of NO to **3**, which lacks the sixth ligand (Table 4). A similar substitution behaviour was noted for the reversible binding of NO to the substrate-free and camphor-bound forms of $P450_{cam}$.[44] However, the activation parameters determined for NO coordination to **4** (Table 4) indicate a different mechanism than that proposed for the reversible binding of NO to substrate-free $P450_{cam}$. Whereas NO binding to the resting form of $P450_{cam}$ is controlled by dissociation of a coordinated water molecule, the displacement of a methanol molecule in **4** follows an associative interchange process in which the volume collapse reflects Fe^{III}–NO bond formation with a concomitant change from a high-spin to low-spin state. As already mentioned, NO coordination to substrate-free $P450_{cam}$ does not involve a high-spin to low-spin rearrangement of the iron(III) centre.[44] These opposite effects are clearly seen by comparison of the volume profiles constructed for these two reactions (Figure 10).

The NO binding constants determined for the enzyme models **3** and **4** are about four orders of magnitude smaller than those found for the native $P450_{cam}$/NO system, which can be explained in terms of the very effective NO dissociation from the nitrosyl complexes of **3** and **4**. Because of the exothermic nature of NO coordination to **3** and **4**, the NO binding constants for these complexes increase significantly with decreasing temperature. This is a general observation noted also for other model enzymes (for instance, the binding of dioxygen to hemocyanine and tyrosinase) where intermediate oxidant or substrate-bound species can be stabilized only at very low temperatures. This feature clearly evidences the important role of the enzyme pocket of $P450_{cam}$ in stabilizing the NO^+ state and in forming more stable nitrosyl complexes at ambient temperature relative to those observed for many protein free model complexes. Thus, although the ligand-substitution behaviour of synthetic iron(III) porphyrin complexes can to some extent be regulated by tuning the electronic nature of the porphyrin ring, by the identity and number of axial ligands and by selection of experimental conditions (coordinating/non-coordinating solvent, pH, temperature, etc.), comparison of the kinetic and thermodynamic data for the native iron(III)-thiolate hemoproteins with those obtained for protein-free enzyme models clearly highlights the unique features of the protein architecture in controlling the dynamics of NO binding to P450 cytochromes according to their physiological activity.

8. Reductive Nitrosylation Reactions of Fe^{III} Porphyrin Complexes

As mentioned in earlier sections, the binding of NO to the iron(III) centres of hemoproteins and model systems results in the formation of nitrosyl products with a linear coordination mode of the Fe–NO bond and significant charge transfer from NO to the metal centre. This leads formally to the one-electron reduction of the Fe^{III} centre

and to the formation of a $(P)Fe^{II}(NO^+)$ complex with a coordinated nitrosyl (NO^+) ligand, which is isoelectronic to carbon monoxide. Clearly, NO^+ as an electrophilic ligand (much more electrophilic than free NO) may be susceptible to nucleophilic attack in aqueous and nonaqueous solution, which can result in the apparent instability of the nitrosyl complexes of iron(III) porphyrins relative to their analogous $(P)Fe^{II}(NO)$ species. Indeed, it has long been known that ferriheme proteins (methemoglobin and ferricytochrome *c*) undergo autoreduction when exposed to NO in aqueous solution.[68] Although many groups have systematically investigated NO reduction processes of various ferriheme proteins,[50,69] the mechanisms of these reactions are still far from completely understood. Hoshino et al.[70] reported detailed kinetic studies on the NO reductions of some ferriheme proteins in buffered solutions at various pH and proposed a plausible reaction sequence for the reductive nitrosylation of iron(III) centres. This involves attack of a nucleophile (Nu), viz. a water molecule or hydroxide ion as a general base, on the ferrous nitrosonium complex to produce a ferrous porphyrin species [which reacts very rapidly with excess NO to give (P)Fe(NO)] and the nitrosylated nucleophile as shown in Scheme 5.

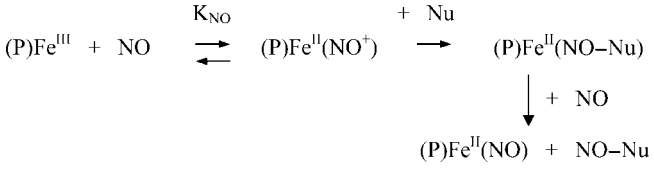

Scheme 5.

This finding has motivated many researchers to study, in detail, the role of general base buffer and hydroxide ion catalysis on the reductive nitrosylation of many ferriheme proteins and iron(III) porphyrin models.[71,72] During the course of these studies, a very important discovery was made that the nitrite ion (present in the reaction medium as a reaction product or as an ubiquitous impurity in aqueous NO solutions) can also be regarded as a catalyst for this reaction.[72] In order to account for the catalytic effect of nitrite, two mechanistic proposals were made.[72] The first involves an inner-sphere pathway proceeding by nucleophilic attack of the nitrite ion on the electrophilic, coordinated NO^+ to produce the iron(II) complex of the N_2O_3 species ($Fe–N_2O_3$) as a key intermediate. Dissociation of this complex followed by subsequent fast reactions [i.e. hydrolysis of N_2O_3 to nitrous acid and very rapid nitrosylation of the iron(II) porphyrin complex] lead to the reaction products and regeneration of catalytic nitrite. Another possible mechanism is described by an outer-sphere electron-transfer process between the nitrite ion and the ferrous nitrosonium complex to give a nitrosyl iron(II) porphyrin and nitrogen dioxide. NO_2 would then react very rapidly with the excess NO to form N_2O_3, which further undergoes hydrolysis to nitrite. Notably, a common aspect of these two mechanisms is the formation of N_2O_3 as a reactive intermediate. In aqueous solution, it can very easily undergo hydrolysis to nitrous acid; however, in the hydrophobic protein pocket, N_2O_3 formed during reductive nitrosylation of ferriheme proteins can offer other possibilities, for example, as an important nitrosating agent for protein amines or thiols.

All these interesting results have inspired us to investigate the reactions of reductive nitrosylation of iron(III) porphyrin models in more detail. Our contribution in this area involves temperature and pressure studies on the reductive nitrosylation reactions following the binding of NO to $(TMPyP^{4+})Fe^{III}(H_2O)_2$ (at pH = 4)[34] and to the highly negatively $[(P^{8-})Fe^{III}]$ and highly positively $[(P^{8+})Fe^{III}]$ charged ferric porphyrins (at high and low pH).[73] Estimation of the activation parameters for the nitrite-catalyzed reductive nitrosylation of these iron(III) models enabled us to discuss the validity of the above-mentioned inner- and outer-sphere mechanisms proposed for the catalytic effect of the NO_2^- ion, as well as allowed us to establish the role of the overall charge on the porphyrin ring and iron centre on the rate and mechanism of reductive nitrosylation reactions.

Nitrite concentration dependence studies of the reaction between the nitrosyl complex of $(TMPyP^{4+})Fe^{III}(H_2O)_2$ and NO_2^- at pH = 4 revealed that positively charged $(TMPyP^{4+})Fe^{II}(H_2O)(NO^+)$ undergoes reductive nitrosylation (in the presence of added nitrite) significantly faster than that already reported for the negatively charged $(TPPS^{4-})Fe^{II}(H_2O)(NO^+)$ complex[72] (Table 5). Activation parameters determined for this reaction are significantly positive (Table 5), which can indicate the significant role of electrostriction effects as a result of charge neutralization during binding of NO_2^- to coordinated NO^+. The substantial contribution of these effects on the rate of reductive nitrosylation processes can be better understood in terms of the more recent results from mechanistic studies on the nitrite-catalyzed reductive nitrosylation of $(P^{8-})Fe^{III}$ and $(P^{8+})Fe^{III}$ complexes.[73] It was shown that exposure of aqueous solutions of $(P^{8-})Fe^{III}(H_2O)_2$ at pH = 7 and of $(P^{8+})Fe^{III}(H_2O)_2$ at pH = 2 leads to rapid nitrosylation reactions to produce $(P^{8-})Fe^{II}(H_2O)(NO^+)$ and $(P^{8+})Fe^{II}(H_2O)(NO^+)$, respectively. The NO binding reaction is, in both cases, followed by the slower subsequent reductive nitrosylation reaction, which leads to the formation of five-coordinate nitrosyl adducts as the final products, $(P^{8-})Fe^{II}(NO)$ and $(P^{8+})Fe^{II}(NO)$, respectively. The NO concentration dependence of the observed rate constant for reductive nitrosylation of these complexes enabled the calculation of the first-order rate constants for the reduction reactions (k_{red}). It was revealed that the value of k_{red} is almost two orders of magnitude larger for the reduction of the positively charged $(P^{8+})Fe^{II}(NO^+)$ species than for that of the negatively charged $(P^{8-})Fe^{II}(NO^+)$ porphyrin. This observation is in line with the results obtained earlier for the reductive nitrosylation of $(TPPS^{4-})Fe^{III}$ and $(TMPyP^{4+})Fe^{III}$[34,72] and can be explained in terms of the electrophilicity of the iron(III) centres in both complexes. The accelerated reductive nitrosylation observed for $(P^{8+})Fe^{II}(NO^+)$ can be ascribed to the higher electrophilicity of

Table 5. Rate constants and activation parameters for the nitrite-catalyzed reductive nitrosylation reactions of $(P)Fe^{II}(H_2O)(NO^+)$ complexes.

Starting complex	pH	k_{nit} (25 °C) [$M^{-1}s^{-1}$]	$\Delta H^{\#}$ [kJ mol^{-1}]	$\Delta S^{\#}$ [J mol^{-1} K^{-1}]	$\Delta V^{\#}$ [cm^3 mol^{-1}]	Ref.
$(P^{8+})Fe(H_2O)_2$	2	155 ± 8	90 ± 3	99 ± 10	7.2 ± 0.5	[73]
$(P^{8+})Fe(H_2O)_2$	4	242 ± 3	73 ± 2	92 ± 7	12.3 ± 0.7	[73]
$(P^{8+})Fe(OH)(H_2O)$	8	22 ± 1	68 ± 1	5 ± 2	2.2 ± 0.2	[73]
$(TMPyP^{4+})Fe(H_2O)_2$	4	159 ± 12	88 ± 2	92 ± 6	8.8 ± 0.1	[34]
$(TMPyP^{4+})Fe(H_2O)_2$	5	83 ± 3	–	–	–	[72]
$(TPPS^{4-})Fe(H_2O)_2$	5	3.1	–	–	–	[72]
$(P^{8-})Fe(H_2O)_2$	7	2.1 ± 0.2	60 ± 2	–36 ± 7	–8.6 ± 0.4	[73]

the metal centre and of coordinated NO^+, which is the result of the presence of the positively charged electron-withdrawing *meso* substituents in the heme environment. Conversely, electron-donating groups in $(P^{8-})Fe^{II}(NO^+)$ seem to stabilize the nitrosyl complex by the increased electron density at the iron(II) centre and therefore slow down the reductive nitrosylation reaction. Similarly, the presence of the OH^- group in the position *trans* to NO^+ in (P^{8+})-$Fe^{II}(OH)(NO^+)$ (at pH = 8) has been shown to reduce k_{red} significantly for this complex, mainly because of the induced electron density (coming from the *trans* OH^- ligand) on the nitrosyl ligand and the decrease in electrophilic character.[73]

Since the reductive nitrosylation reactions observed for the above systems can be catalyzed by nitrite ions present in the solution as a final reaction product, a detailed study of the nitrite-catalyzed reduction of $(P^{8-})Fe^{II}(NO^+)$ and $(P^{8+})Fe^{II}(NO^+)$ was performed.[73] The values of the reduction rate constant with nitrite ion as catalyst (k_{nit}) obtained for these complexes and related systems are summarized in Table 5.

During the course of these studies, it was revealed that the rates of reductive nitrosylation are sensitive to the nature of the reactant, viz. HONO or NO_2^- [see for example the rate constants determined for the $(P^{8+})Fe(H_2O)_2$ complex at pH = 2 and 4, where nitrous acid exists mainly as HONO and NO_2^-, respectively], and to the protonated/deprotonated form of the coordinated water molecule [see rate constants determined for $(P^{8+})Fe(H_2O)_2$ and (P^{8+})-$Fe(OH)(H_2O)$ at pH = 4 and 8, respectively]. All these observations indicate that nitrite-catalyzed reductive nitrosylation of the complexes studied proceeds according to an inner-sphere mechanism described by direct nucleophilic attack of the $HONO/NO_2^-$ species on coordinated NO^+ to form the Fe^{II}–N_2O_3 complex, which subsequently dissociates N_2O_3 and rapidly binds NO (present in excess in solution) to form the final product $(P)Fe^{II}(NO)$. Such a mechanism is also strongly supported by the activation parameters determined for k_{nit} (Table 5). Activation entropies and activation volumes for the nitrite-catalyzed reductive nitrosylation of cationic complexes are substantially positive, whereas those for the negatively charged porphyrin complexes are significantly negative. This correlates very well with the electrophilicity of coordinated NO^+, which in turn controls the contribution of changes in electrostriction that accompanies bond formation between the electrophilic nitrosonium ligand and the $HONO/NO_2^-$ species. For example, the electrophilicity of the NO^+ ligand in (P^{8-})-$Fe^{II}(H_2O)(NO^+)$ is not expected to be high because of the overall negative charge on the porphyrin ring, such that charge neutralization and decrease in the electrostriction during bond formation is relatively small in comparison to the intrinsic contributions arising from bond formation. This means that positive contributions to the activation entropy and activation volume arising from the decrease in electrostriction (accompanied by the release of solvent molecules) can only partially compensate the negative intrinsic contributions associated with bond formation, which finally leads to the substantially negative values of the activation parameters and relatively small value of k_{nit}. In contrast, bond formation between $HONO/NO_2^-$ and the highly electrophilic NO^+ in $(P^{8+})Fe^{II}(H_2O)(NO^+)$ (because of the additional positive charge on the heme environment) will result in more effective charge neutralization. Thus, in this case, the positive contributions arising from the significant decrease in electrostriction are expected to play a major role. This is reflected by the substantially positive values for the activation parameters and high k_{nit} values found for this system. In summary, the observed trend in the k_{nit} values for a series of $(P^n)Fe^{III}$ complexes [$(P^{8+})Fe^{III}$ > $(TMPyP^{4+})$-Fe^{III} > $(TPPS^{4-})Fe^{III}$ > $(P^{8-})Fe^{III}$] along with the activation parameters determined for these systems strongly support the operation of an inner-sphere electron-transfer mechanism for the reductive nitrosylation reactions of iron(III) porphyrins, as opposed to an outer-sphere electron-transfer mechanism, which was proposed in recent reports.[71c,72]

9. Reductive Nitrosylation of Water-Soluble Cobalt Porphyrins

Vitamin B_{12a}, aquacobalamin [$Cbl(H_2O)$], was proposed to react with NO under biological conditions and to regulate its physiological functions in this way.[74] Experimental and theoretical work from our laboratory proved that $Cbl(H_2O)$ does not react with NO at pH 7.[75,76] Nevertheless, it was reported later that $Cbl(H_2O)$ reacts with NO at low pH, under conditions in which the dimethylbenzimidazole group is protonated and subsequently dechelates.[77] The final product of this reaction was not a Co^{III}–(NO) complex but Co^{II}–(NO), or better described as Co^{III}–(NO^-). This complex is also obtained when reduced $Cbl(H_2O)$ reacts with NO;[78] in this way, the reaction is a reductive nitrosylation process. Co porphyrins react in a

manner similar to that for Cbl(H_2O) at low pH, generating Co^{III}–(NO^-) complexes as final products.[33c,79] In this way, the reaction under study can be described by reaction (9).

$$Co^{III}(P) + 2\,NO \rightarrow\!\!\rightarrow Co^{III}(P)(NO^-) + NO_2^- \quad (9)$$

From titrations of the $[Co^{III}(TPPS)(H_2O)_2]^{3-}$ complex solution with NO, the stoichiometry of the consumption of NO was determined to be close to 2. Quantification of the NO_2^- concentration at the end of the reaction allowed us to conclude that approximately 1 mol of NO_2^- is produced per mol of complex, which gives strong support to the overall stoichiometry described by reaction (9).[80]

Three different Co-porphyrin complexes were studied [TPPS, TMPyP and TCPP = *meso*-tetra(4-carboxyphenyl)-porphyrin]; all of them react with NO and show, qualitatively, a very similar picture.[80] The reactivity difference correlates with the electron density on the metal centre. The reaction with NO proceeds through an apparently single first-order reaction; however, the isosbestic points are not clean, the observed rate constants are not reproducible and, in some cases, the kinetic traces had to be fitted to a two-exponential function. These findings suggest a more complex behaviour. For this reason the influence of NO_2^-/HNO_2 on the kinetics was studied in detail, since these species are typical and unavoidable impurities in aqueous NO solutions.[72c,75] The reactions of the three complexes under study were strongly pH dependent. At pH > 3, two reaction steps were clearly observed, whereas at pH < 3, a single reaction step was observed.

At pH < 3, in contrast to the behaviour at higher pH, formation of the final product is observed from the beginning of the reaction. The kinetic data show that the reaction is controlled by the reversible substitution of coordinated water to produce the $[Co^{III}(P)(NO)(H_2O)]$ complex, i.e. the product of the primary interaction between NO and the starting compound.[80] A weak EPR signal obtained at pH 1 with a $[Co(TPPS)(H_2O)_2]^{3-}$ sample saturated with NO gives some evidence for the presence of this intermediate.[80,81c] These complexes were obtained by electrochemical methods in organic solvents and characterized in situ,[81] since they are very unstable towards NO dissociation, to generate $[Co(P)(solvent)_2]$ complexes.[81b] We propose that the $[Co^{III}(P)(NO)(H_2O)]$ complex reacts with a second NO molecule to generate the dinitrosyl species $[Co^{III}(P)(NO)_2]$ (see left side of Scheme 6). This compound produces the final product through an inner-sphere electron-transfer reaction. These $[Co(P)(L)_2]$ compounds were observed for all the ligands studied, viz. SCN^-, I^-, pyridine.[82] Moreover, we observed the formation of $[Co(P)(NO_2^-)_2]$ complexes.[80] In all of these cases, the coordination of the second ligand molecule is faster than that of the first because of the increase in electron density on the metal centre, which is in agreement with the fact that coordination of the first NO molecule is the rate-determining step and with the observation of a single reaction step.

At pH > 3, two reactions were clearly observed when mixtures of NO and NO_2^- were used. It was concluded that the first reaction is controlled by the competition between these two species to substitute one of the coordinated water molecules in the complex.[80] In this way, the expression of the observed rate constant for this reaction ($k_{1(obs)}$) can be written as in Equation (10) [see Figure 12].

$$k_{1(obs)} = k_{NO}[NO] + k_{NO_2^-}[NO_2^-] \quad (10)$$

The values of k_{NO} obtained at pH 1 are in agreement with those obtained at higher pH in the presence of NO_2^-. This is also true for the values of $k_{NO_2^-}$ obtained in the absence and presence of NO (see Figure 12). The proposed rate law in Equation (10) is supported by the kinetic data and activation parameters obtained for the first reaction step at pH 5 and 1 and is in agreement with the data reported in the literature for the reaction of the same Co(P)

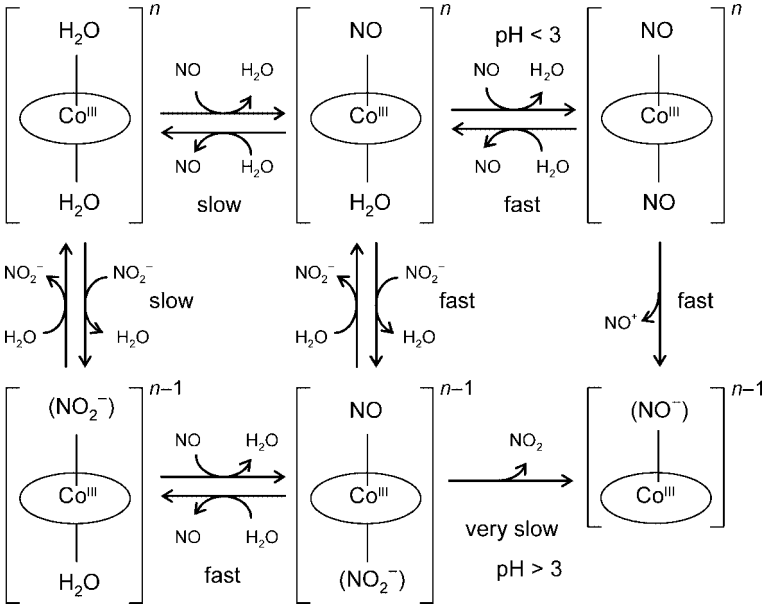

Scheme 6.

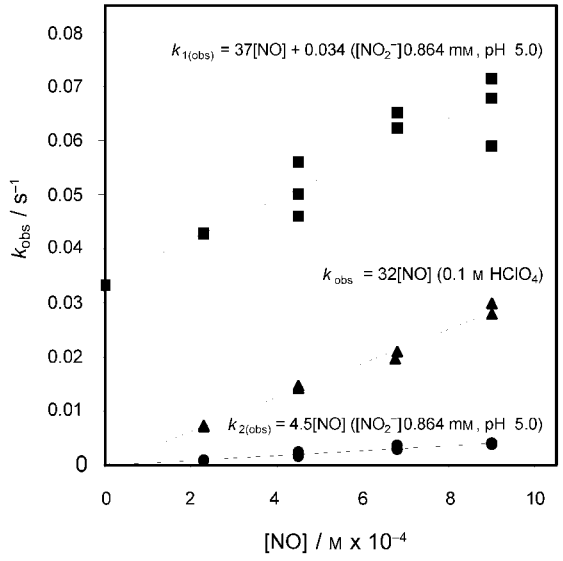

Figure 12. NO concentration dependence for the reaction with $[Co(TPPS)(H_2O)_2]^{3-}$ studied under different conditions: pH = 5.0 (0.01 M acetate buffer) or pH = 1.0 ($HClO_4$), I = 0.1 M ($NaClO_4$), T = 25.0 °C, $[Co(TPPS)(H_2O)_2^{3-}]$ = 1–5 × 10^{-6} M. Different values of k_{obs} represent the spread in the measurements at a particular NO concentration (each data point is the average of 4 to 10 kinetic runs).

complexes with other ligands (see Table 6 and Table 7).[82] The first reaction step for the three complexes correlates with the electron density on the metal centre as was previously observed. The spectrum of the intermediate generated during the reaction was very similar to that of the $[Co(P)(NO_2^-)(H_2O)]$ complex; no final product, i.e. $[Co^{III}(P)(NO^-)]$, was produced and no EPR signals could be detected either. According to Equation (10), the $[Co(P)(NO_2^-)(H_2O)]$ and $[Co(P)(NO)(H_2O)]$ complexes should be the products of the first reaction, where NO_2^- and NO compete. Nevertheless, only the first compound was detected. We propose that the second intermediate is unstable under these conditions, even more than at pH 1, and the presence of NO_2^- leads to the decomposition of this intermediate thus releasing NO and generating $[Co(P)(NO_2^-)(H_2O)]$ (see central part of Scheme 6). This decomposition of the intermediate by NO_2^- is prevented at low pH through protonation, where formation of the final product is observed from the beginning of the reaction.

The second reaction was observed at pH > 3. The observed rate constants for this reaction ($k_{2(obs)}$) are very similar to those observed for the reaction between the $[Co(P)(NO_2^-)(H_2O)]$ complexes and NO under similar conditions. On the other hand, they do not depend significantly on the NO_2^- concentration, they depend linearly on the NO concentration (see Figure 12) and the activation parameters support a dissociative mechanism. The nature of this reaction is discussed elsewhere, and several possible mechanisms are considered, among them the oxo-transfer reaction.[80] We propose that the $[Co(P)(NO_2^-)(H_2O)]$ complex is, in the presence of NO, in equilibrium with small amounts of the $[Co(P)(NO_2^-)(NO)]$ intermediate (see lower part of Scheme 6). This last intermediate slowly decomposes through an inner-sphere electron-transfer reaction to generate the final product $[Co^{III}(P)(NO^-)]$ and NO_2. Thus, this reaction would be the rate-determining step for the second reaction. This proposal is consistent with the NO- and NO_2^- concentration dependences, as well as with the activation parameters.

In the reductive nitrosylation of Fe^{III} porphyrins, where general base catalysis was observed, it was proposed that the $[Fe^{III}(P)NO]$ complex is attacked by nucleophiles such as NO_2^-, different bases and even solvents to generate the $Fe^{II}(P)$ complex.[71,72] The latter complex reacts under diffusion-controlled conditions with NO to produce the final product. We do not have any evidence in favour of such catalysis in our system. If this was the case, we would expect different NO_2^- concentration- and pH dependences. We believe that the reason why reductive nitrosylation of Co porphyrins is so different from that of the Fe analogues is the instability of the $[Co^{III}(P)(NO)(H_2O)]$ intermediate.[80,81] Although the electronic structure of this compound may have some contribution from the $[Co^{II}(P)(NO^+)(H_2O)]$

Table 6. Kinetic data for reactions of NO and NO_2^- with the $[Co(TPPS)(H_2O)_2]^{3-}$ complex.[a]

Reaction	k_1 [$M^{-1}s^{-1}$] [Intercept, s^{-1}]	k_2 [$M^{-1}s^{-1}$] [Intercept, s^{-1}]	$\Delta H^{\neq}_1$ kJ mol^{-1}	$\Delta H^{\neq}_2$ kJ mol^{-1}	$\Delta S^{\neq}_1$ J K^{-1} mol^{-1}	$\Delta S^{\neq}_2$ J K^{-1} mol^{-1}	$\Delta V^{\neq}_1$ cm^3 mol^{-1}	$\Delta V^{\neq}_2$ cm^3 mol^{-1}
NO (pH 1.0)	32 ± 1		101 ± 2		+121 ± 6		+13 ± 1	
NO_2^- (pH 5.0)	38.5 ± 0.8		90.2 ± 0.6		+88 ± 2		+11 ± 1	
HNO_2 (pH 1.0)	14.2 ± 0.4 [(7 ± 1) × 10^{-3}]		93 ± 2		+91 ± 5		+15 ± 1	
NO ([NO_2^-] 1 mM, pH 5.0)	37 ± 5 [(3.4 ± 0.4) × 10^{-2}]	4.5 ± 0.5	94 ± 3	98 ± 3	+100 ± 10	+97 ± 9	+13 ± 1	+14 ± 1
NO_2^- ([NO] 0.9 mM, pH 5.0)	41 ± 4 [(3.0 ± 0.4) × 10^{-2}]	[(4.2–3.2) × 10^{-3}]						
HNO_2 ([NO] 0.9 mM, pH 1.0)	13 ± 1 [(3.4 ± 0.5) × 10^{-2}]							
SCN^-	179[b]		77[c]		+60[c]		+15.4[d]	
Py	520[b]		74[c]		+60[c]			
I^-	118[c]		87[c]		+87[c]			

[a] I = 0.1 M, unless otherwise stated; subscripts 1 and 2 refer to the first and second observed reaction steps. [b] From ref.[82a] [c] From ref.[82b] I = 1.0 M. [d] from ref.[82h] I = 1.0 M.

Table 7. Kinetic data for the different Co^{III} porphyrin complexes studied.[a]

Reaction	$[Co(TPPS)(H_2O)_2]^{3-}$		$[Co(TCPP)(H_2O)_2]^{3-}$		$[Co(TMPyP)(H_2O)_2]^{5+}$	
	k_1 [$M^{-1}s^{-1}$] [Intercept, s^{-1}]	k_2 [$M^{-1}s^{-1}$] [Intercept, s^{-1}]	k_1 [$M^{-1}s^{-1}$] [Intercept, s^{-1}]	k_2 [$M^{-1}s^{-1}$] [Intercept, s^{-1}]	k_1 [$M^{-1}s^{-1}$] [Intercept, s^{-1}]	k_2 [$M^{-1}s^{-1}$] [Intercept, s^{-1}]
NO (pH 1.0)	32 ± 1				$(1.5 \pm 0.1) \times 10^{-1}$	
NO_2^-	38.5 ± 0.8[b]		54.1 ± 0.2[c]		8.4 ± 0.2[d]	
HNO_2 (pH 1.0)	14.2 ± 0.4 $[(7 \pm 1) \times 10^{-3}]$					
NO ([NO_2^-] 1 mM)	37 ± 5[b] $[(3.4 \pm 0.3) \times 10^{-2}]$	4.5 ± 0.5[b]	130 ± 10[c] $[(5.3 \pm 0.1) \times 10^{-2}]$	7.2 ± 0.5[c]	1.6 ± 0.2[d] $[(8.4 \pm 0.1) \times 10^{-3}]$	2.2 ± 0.3[d]
NO_2^- ([NO] 0.9 mM)	41 ± 4[b] $[(3.0 \pm 0.4) \times 10^{-2}]$	$[(3.2–4.2) \times 10^{-3}]$	47 ± 6[c] $[(1.2 \pm 0.1) \times 10^{-1}]$	$[(5.3–6.7) \times 10^{-3}]$	8.8 ± 0.8[d]	$[(1.6–2.4) \times 10^{-3}]$
SCN^-	179[e]		450[g]		2.1[h]	
Py	520[e]		1400[g]		0.7[h]	
I^-	118[f]				1.6[i]	
pK_a	7.0[f]		7.5[g]		6.0[h]	

[a] T = 25.0 °C, I = 0.1 M, unless otherwise stated; subscripts 1 and 2 refer to the first and second observed reaction steps. [b] pH 5.0. [c] pH 6.0. [d] pH 4.7. [e] From ref.[82a] [f] From ref.[82b] I = 1.0 M. [g] From ref.[82g] I = 0.5 M. [h] From ref.[82d] I = 0.5 M. [i] From ref.[82f] I = 1.0 M.

structure, its instability prevents any further reaction with nucleophiles. In fact, such reactions are quite slow and they are about 10^{-3} s^{-1} for the reactions with solvent (water), acetate, etc.[71,72]

10. Reductive Nitrosylation of Aquacobalamin at Low pH

As mentioned in the previous section, aquacobalamin, [Cbl(H_2O)], does not react with NO at pH 7,[75,76] nevertheless, it was reported that it can undergo reductive nitrosylation at low pH to generate a Co^{III}–NO^- complex or Cbl(NO^-)[77] in a manner similar to that of Co porphyrins.[79] As a natural extension of the kinetic and mechanistic studies on Co porphyrins,[80] the reductive nitrosylation of Cbl(H_2O) at low pH was revisited.[83] Many similarities between Cbl(H_2O) and the previously studied Co porphyrins, as well as some important differences, were found.

In the preliminary experiments, kinetic traces obtained during the reaction with NO were irreproducible, which shows, in many cases, a more complex behaviour than a simple first-order process. The influence of HNO_2 impurities was studied by using mixtures of NO and HNO_2. As previously found for Co porphyrins, two reaction steps were observed. The first reaction shows very small absorption changes and proceeds on the stop-flow timescale. The UV/Vis spectrum of the intermediate generated during the first reaction is very similar to that of the Cbl(NO_2^-) complex generated for the same HNO_2 concentration. The observed rate constants obtained for this reaction ($k_{1(obs)}$) are independent of the NO concentration. On the other hand, they show a linear dependence on the HNO_2 concentration with a slope of 110 ± 2 $M^{-1}s^{-1}$ and an intercept of $(4.0 \pm 0.2) \times 10^{-2}$ s^{-1}. Very similar parameters were obtained if no NO (only HNO_2) is present in the medium, i.e. 106 ± 5 $M^{-1}s^{-1}$ and 3.3 ± 0.6 s^{-1}, respectively. In other words, NO does not react with Cbl(H_2O) even at pH 1.[83]

The second reaction step shows the spectral changes reported in the literature for the reductive nitrosylation of Cbl(H_2O) at low pH, and the Cbl(NO^-) complex is produced as final product.[77] It was previously reported that this reaction was independent of the NO concentration.[77] We found, however, that the observed rate constant for this reaction ($k_{2(obs)}$) depends on the NO and HNO_2 concentrations, but the dependence on the concentration of each species is quite surprising and unexpected.[83] For example, when the HNO_2 concentration was kept constant, the $k_{2(obs)}$ values decreased with increasing NO concentration. As the yield of the reaction decreased as the NO concentration decreased, quantitative information was not obtained. On the other hand, when the NO concentration was kept constant, the $k_{2(obs)}$ values increased with increasing HNO_2 concentration, and a non-linear, quadratic dependence was observed (see Figure 13). The yield of the final product decreased also when the HNO_2 concentration increased, which is in agreement with the previous finding. The second reaction step is strongly pH dependent. As was previously reported, the reaction rate decreases with increasing pH, and the reaction is no longer observed at pH > 4.[77] The pH dependence correlates with the spectral changes observed for the Cbl(NO_2^-) complex as a function of pH. From the UV/Vis data, the pK_a of the protonated Cbl(NO_2^-) complex is estimated to be close to 1.[83] In contrast, the pK_a of protonated Cbl(H_2O) is –2.5.[84] We propose that the dimethylbenzimidazole group is protonated at low pH and dissociates from the metal centre to leave a vacant site for the coordination of NO. The dissociation of this group after protonation is a fast reaction [ca. 0.3 s^{-1} at pH 1 for the Cbl(NO_2^-) complex].[83] In this way, the reactive species towards NO is not Cbl(H_2O) but the Cbl(NO_2^-) complex (see Scheme 7), since the concentration of the protonated form of Cbl(H_2O) is extremely low at pH 1.

The effect of the HNO_2 concentration on $k_{2(obs)}$ and on the yield of the reaction revealed the possibility of a reaction between HNO_2 and the Cbl(NO^-) complex, i.e. a *back reaction*. Interestingly, the observed rate constants for this last reaction (k_{obs}) do not differ significantly from $k_{2(obs)}$ obtained for identical HNO_2 and NO concentrations (see

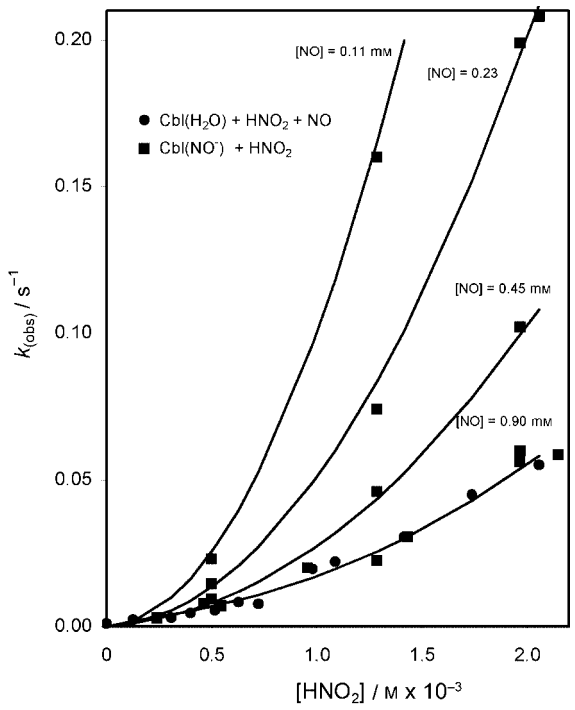

Figure 13. $[HNO_2]$ dependence of the observed rate constant for the second reaction step ($k_{2(obs)}$) and of the reaction between $Cbl(NO^-)$ and HNO_2 (k_{obs}). The solid line corresponds to the simulated data according to Equation (12), by using K_{HNO_2} = 2800 M^{-1} (fixed variable), $k_{NO} = 7 \pm 2$ $M^{-1} s^{-1}$ and $K = 0.6 \pm 0.2$. Experimental conditions: pH = 1.0, I = 0.1 M ($HClO_4$), T = 25.0 °C. $[Cbl(H_2O)]$ = 0.01–0.05 mM.

Figure 13).[83] Moreover, k_{obs} values show a quadratic dependence on the HNO_2 concentration and decrease when the NO concentration increases. The product of the *back reaction* must be $Cbl(NO_2^-)$ in equilibrium with $Cbl(H_2O)$, since HNO_2 is in excess and no consecutive reactions are observed. In this way, the reductive nitrosylation is a reversible reaction and can be expressed by reaction (11).

$$Cbl(NO_2^-) + 2\,NO + H_2O \rightleftharpoons Cbl(NO^-) + 2\,HNO_2;\ K \qquad (11)$$

According to the kinetic data and the earlier work on Co porphyrins, the proposed mechanism for the reaction of $Cbl(H_2O)$ with NO at low pH is summarized in Scheme 7.

According to this mechanism and the assumptions described elsewhere,[83] Equation (12) can be derived, where K_{HNO_2} is the equilibrium constant for the formation of the $Cbl(NO_2^-)$ complex, K is the equilibrium constant for the reductive nitrosylation expressed in reaction (11) and k_{NO} expresses the rate constant for the release of NO_2^- from the $Cbl(NO_2^-)(NO)$ intermediate (see Scheme 7), which is the rate-determining step in the second reaction step.

$$k_{2(obs)} = \frac{K_{HNO_2}[HNO_2]}{1 + K_{HNO_2}[HNO_2]}\, k_{NO}[NO] + \frac{k_{NO}[HNO_2]^2}{K\,[NO]} \qquad (12)$$

Equation (12) can account for the dependence of $k_{2(obs)}$ for the reductive nitrosylation and of k_{obs} for the *back reaction* on the NO and HNO_2 concentrations. Moreover, by fitting the experimental data with this equation, the values of 7 ± 2 $M^{-1} s^{-1}$ and 0.6 ± 0.2 were obtained for k_{NO} and K, respectively. This latter parameter was confirmed by direct equilibrium measurements.[83] These measurements were also consistent with the stoichiometry expressed in reaction (11). In summary, the reductive nitrosylation is dominated by its *back reaction*, and this is the reason for its strange NO- and HNO_2 concentration dependences.

DFT calculations were performed on the present system.[83] Earlier studies concluded that $Cbl(H_2O)$ cannot interact with NO in aqueous solution.[76] The more recent work focused on the effect of the coordination of NO, NO_2^-, H_2O and OH^- on the lengthening of the Co–dimethylbenzimidazole bond.[83] On deprotonation of the coordinated water molecule in the $Cbl(H_2O)$ complex, significant lengthening of the Co–dimethylbenzimidazole bond occurs. A similar effect is observed upon coordination of NO_2^-. On the other hand, the Co–dimethylbenzimidazole bond length in the Cbl(NO) complex is similar to that in $Cbl(H_2O)$. In this way, lengthening of the Co–dimethylbenzimidazole bond in the $Cbl(NO_2^-)$ complex allows its protonation and dechelation at low pH. This is evidently not possible for the $Cbl(H_2O)$ and Cbl(NO) complexes.

In conclusion, we confirmed that $Cbl(H_2O)$ cannot react with NO even at low pH. We propose that the active species towards NO is $Cbl(NO_2^-)$ and not $Cbl(H_2O)$. A mechanism based on (and consistent with) previous work on Co porphyrins is proposed. This mechanism accounts for the NO- and HNO_2 concentration dependences of the observed rate constant for the reductive nitrosylation ($k_{2(obs)}$) as well as for the pH dependence. As we mentioned in the previous section, Co^{III}–(NO) complexes are very unstable compounds.[81] This is the main reason why the reductive nitrosylation in Co porphyrins is so different from that in the Fe analogues.[71,72] This instability of the Co^{III}–(NO) complexes determines why $Cbl(H_2O)$ does not react with NO as well.[76,83]

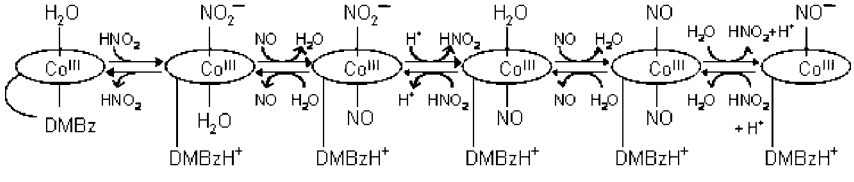

Scheme 7.

11. Conclusions and Future Outlook

The work summarized in this microreview has greatly assisted the mechanistic clarification of the interaction of NO with Fe and Co complexes and of the observed subsequent reactions. It forms an excellent basis for the clarification of observations in the literature that are of significant biological and environmental importance. In this process the application of volume-profile analysis has been extremely useful, especially in cases where the activation of NO is accompanied by changes in the spin state of the metal centre. Presently, we are extending this work to water-soluble model complexes of P450 that closely resemble the coordination environment of P450. Although NO is a radical, the presented work clearly shows that it behaves like any other nucleophile, with the exception that once it is bound to the metal centre there is a redistribution of charge density, which results in a formal redox reaction. Furthermore, the fundamental work involving the binding of NO to P450 and model complexes forms a basis for the understanding of the more complex reaction sequences observed during the activation of peroxides by such systems, a topic that is now being studied in more detail in our group.

Acknowledgments

We gratefully acknowledge financial support from the National Research Council of Argentina (CONICET) and the Deutsche Forschungsgemeinschaft within SFB 583 on "Redox-Active Metal Complexes". We appreciate the productive collaboration with Norbert Jux (Institute for Organic Chemistry, University of Erlangen-Nürnberg).

[1] J. H. Enemark, R. D. Feltham, *Coord. Chem. Rev.* **1974**, *13*, 339.
[2] M. Wolak, R. van Eldik, *Coord. Chem. Rev.* **2002**, *230*, 263.
[3] A. Wanat, T. Schneppensieper, G. Stochel, R. van Eldik, B. Eckhard, K. Wieghardt, *Inorg. Chem.* **2002**, *41*, 4.
[4] T. Schneppensieper, S. Finkler, A. Czap, R. van Eldik, M. Heus, P. Nieuwenhuizen, C. Wreesman, W. Abma, *Eur. J. Inorg. Chem.* **2001**, 491.
[5] T. Schneppensieper, A. Wanat, G. Stochel, R. van Eldik, *Inorg. Chem.* **2002**, *41*, 2565.
[6] a) D. H. Macartney, *Rev. Inorg. Chem.* **1988**, *9*, 101; b) L. M. Baraldo, P. Forlano, A. R. Parise, L. D. Slep, J. A. Olabe, *Coord. Chem. Rev.* **2001**, *219–221*, 881; c) A. G. Sharpe, *The Chemistry of Cyano Complexes of the Transition Metals*, Academic Press, London, **1976**.
[7] a) H. E. Toma, J. M. Malin, *Inorg. Chem.* **1974**, *13*, 1772; b) H. E. Toma, *Inorg. Chim. Acta* **1975**, *15*, 205; c) H. E. Toma, A. A. Batista, H. B. Gray, *J. Am. Chem. Soc.* **1982**, *104*, 7509; d) I. Maciejowska, R. van Eldik, G. Stochel, Z. Stasicka, *Inorg. Chem.* **1997**, *36*, 5409; e) H. E. Toma, N. M. Moroi, N. Y. M. Iha, *An. Acad. Brasil. Cienc.* **1982**, *54*, 315; f) H. E. Toma, J. M. Malin, E. Giesbrecht, *Inorg. Chem.* **1973**, *12*, 2084; g) E. H. Toma, J. M. Malin, *Inorg. Chem.* **1973**, *12*, 1039; h) H. E. Toma, J. M. Malin, *Inorg. Chem.* **1973**, *12*, 2080; i) H. E. Toma, J. M. Martins, E. Giesbrecht, *J. Chem. Soc., Dalton Trans.* **1981**, 1610.
[8] a) R. Nast, J. Schmidt, *Angew. Chem. Int. Ed. Engl.* **1969**, *8*, 383; b) J. D. W. van Voorst, P. Hemmerich, *J. Chem. Phys.* **1966**, *45*, 3914; c) J. R. Bertolino, C. O. Della Védova, O. Sala, *Polyhedron* **1989**, *8*, 361; d) J. Masek, E. Maslova, *Collection Czechoslov. Chem. Commun.* **1974**, *39*, 2141.
[9] R. P. Cheney, M. G. Simic, M. Z. Hoffman, I. A. Taub, K. D. Asmus, *Inorg. Chem.* **1977**, *16*, 2187.
[10] a) M. J. Clarke, J. B. Gaul, *Struct. Bonding (Berlin)* **1993**, *81*, 147; b) A. R. Butler, C. Glidewell, *Chem. Soc. Rev.* **1987**, *16*, 361.
[11] F. Roncaroli, J. A. Olabe, R. van Eldik, *Inorg. Chem.* **2003**, *42*, 4179.
[12] a) F. Roncaroli, R. van Eldik, J. A. Olabe, *Inorg. Chem.* **2005**, *44*, 2781; b) The $[Fe(CN)_5NO]^{3-}$ complex reacts with NO to generate nitroprusside. The $[Fe(CN)_4NO]^{2-}$ complex is responsible for this behaviour, which can be prevented by the addition of CN^-. These reactions are discussed in ref.[12a]
[13] C. H. Langford, H. B. Gray, *Ligand Substitution Processes*, W. A. Benjamin, Inc., **1965**.
[14] G. Stochel, J. Chatlas, P. Martínez, R. van Eldik, *Inorg. Chem.* **1992**, *31*, 5480.
[15] T. W. Swaddle, *Inorg. Chem.* **1983**, *22*, 2663.
[16] M. I. Finston, H. G. Drickamer, *J. Phys. Chem.* **1981**, *85*, 50.
[17] J. Legros, *J. Chim. Phys. Phys.-Chim. Biol.* **1964**, *61*, 909.
[18] S. Alsheri, J. Burgess, *Inorg. Chim. Acta* **1991**, *181*, 153.
[19] T. R. Sullivan, D. R. Stranks, J. Burgess, R. I. Haines, *J. Chem. Soc., Dalton Trans.* **1977**, 1460.
[20] M. J. Blandamer, J. Burgess, K. W. Morcom, R. Sherry, *Transition Met. Chem.* **1983**, *8*, 354.
[21] G. Stochel, R. van Eldik, E. Hejmo, Z. Stasicka, *Inorg. Chem.* **1988**, *27*, 2767.
[22] a) A. D. James, R. S. Murray, *J. Chem. Soc., Dalton Trans.* **1977**, 326; b) A. D. James, R. S. Murray, W. C. E. Higginson, *J. Chem. Soc., Dalton Trans.* **1974**, 1273.
[23] G. Stochel, R. van Eldik, *Inorg. Chim. Acta* **1991**, *190*, 55.
[24] F. Roncaroli, J. A. Olabe, R. van Eldik, *Inorg. Chem.* **2002**, *41*, 5417.
[25] I. Maciejowska, Z. Stasicka, G. Stochel, R. van Eldik, *J. Chem. Soc., Dalton Trans.* **1999**, 3643.
[26] A. Wanat, R. van Eldik, G. Stochel, *J. Chem. Soc., Dalton Trans.* **1998**, 2497.
[27] P. C. Ford, L. E. Laverman, *Coord. Chem. Rev.* **2005**, *249*, 391.
[28] J. R. Stone, M. A. Marletta, *Biochemistry* **1994**, *33*, 5636.
[29] K. Nakahara, K. Tanimoto, K. Hatano, K. Usuda, H. Shoun, *J. Biol. Chem.* **1993**, *268*, 8350.
[30] a) R. Cassoly, Q. H. Gibson, *J. Mol. Biol.* **1975**, *91*, 301; b) E. G. Moore, Q. H. Gibson, *J. Biol. Chem.* **1976**, *251*, 2788; c) P. Ascenzi, M. Colleta, R. Santucci, F. Polizio, A. Desideri, *J. Inorg. Biochem.* **1994**, *53*, 273; d) M. Hoshino, K. Ozawa, H. Seki, P. C. Ford, *J. Am. Chem. Soc.* **1993**, *115*, 9568.
[31] J. F. Andersen, X. D. Ding, C. Balfour, T. K. Shokhireva, D. E. Champagne, F. A. Walker, W. R. Montfort, *Biochemistry* **2000**, *39*, 10118.
[32] a) W. R. Scheidt, M. K. Ellison, *J. Am. Chem. Soc.* **2001**, *123*, 6314; b) P. C. Ford, I. M. Lorkovic, *Chem. Rev.* **2002**, *102*, 993 and references cited therein; c) P. C. Ford, L. E. Laverman, I. M. Lorkovic, *Adv. Inorg. Chem.* **2003**, *54*, 2003 and references cited therein.
[33] a) M. Hoshino, K. Ozawa, H. Seki, P. C. Ford, *J. Am. Chem. Soc.* **1993**, *115*, 9568; b) L. E. Laverman, M. Hoshino, P. C. Ford, *J. Am. Chem. Soc.* **1997**, *119*, 12663; c) L. E. Laverman, P. C. Ford, *J. Am. Chem. Soc.* **2001**, *123*, 11614.
[34] A. Theodoridis, R. van Eldik, *J. Mol. Catal. A* **2004**, *224*, 197.
[35] M. Hoshino, L. Laverman, P. C. Ford, *Coord. Chem. Rev.* **1999**, *187*, 75 and references cited therein.
[36] a) P. A. Duffin, L. F. Larkworthy, J. Mason, A. N. Stephens, R. M. Thompson, *Inorg. Chem.* **1987**, *26*, 2034; b) Y. Chen, F. Lin, R. E. Shepherd, *Inorg. Chem.* **1999**, *38*, 973; c) D. S. Bohle, Ch. Hung, B. D. Smith, *Inorg. Chem.* **1998**, *37*, 5798.

[37] W. R. Scheidt, M. K. Ellison, *Acc. Chem. Res.* **1999**, *32*, 350 and references cited therein.
[38] T. Schneppensieper, A. Zahl, R. van Eldik, *Angew. Chem. Int. Ed.* **2001**, *40*, 1678.
[39] D. M. Guldi, G. M. A. Rahman, N. Jux, D. Balbinot, U. Hartnagel, N. Tagmatarchis, M. Prato, *J. Am. Chem. Soc.* **2005**, *127*, 9830.
[40] J.-E. Jee, S. Eigler, F. Hampel, N. Jux, M. Wolak, A. Zahl, G. Stochel, R. van Eldik, *Inorg. Chem.* **2005**, *44*, 7717.
[41] J.-E. Jee, M. Wolak, D. Balbinot, N. Jux, A. Zahl, R. Van Eldik, *Inorg. Chem.* **2006**, *45*, 1326.
[42] a) W. R. Scheidt, Ch. A. Reed, *Chem. Rev.* **1981**, *81*, 543; b) W. R. Scheidt, S. R. Osvath, Y. J. Lee, Ch. A. Reed, B. Shaevitz, G. P. Gupta, *Inorg. Chem.* **1989**, *28*, 1591; c) D. R. Evans, Ch. A. Reed, *J. Am. Chem. Soc.* **2000**, *122*, 4660 and references cited therein.
[43] M. Wolak, R. van Eldik, *J. Am. Chem. Soc.* **2005**, *127*, 13312.
[44] A. Franke, G. Stochel, C. Jung, R. van Eldik, *J. Am. Chem. Soc.* **2004**, *126*, 4181.
[45] L. E. Laverman, A. Wanat, J. Oszajca, G. Stochel, P. C. Ford, R. van Eldik, *J. Am. Chem. Soc.* **2001**, *123*, 285.
[46] A. Wanat, M. Wolak, Ł. Orzeł, M. Brindell, R. van Eldik, G. Stochel, *Coord. Chem. Rev.* **2002**, *229*, 37 and references cited therein.
[47] a) A. Drljaca, C. D. Hubbard, R. van Eldik, T. Asano, M. V. Basilevsky, W. J. le Noble, *Chem. Rev.* **1998**, *98*, 2167; b) L. Helm, A. E. Merbach, *J. Coord. Chem.* **1999**, *187*, 151.
[48] A. M. Rich, R. S. Armstrong, P. J. Ellis, P. A. Lay, *J. Am. Chem. Soc.* **1998**, *120*, 10827.
[49] a) M. L. Calrson, R. Regen, E. Elber, H. Li, G. N. Phillips, J. L. Olson, Q. H. Gibson, *Biochemistry* **1994**, *33*, 10597; b) T. G. Traylor, D. Magde, J. Marsters, K. Jongeward, G. Wu, K. Walda, *J. Am. Chem. Soc.* **1993**, *115*, 4808.
[50] T. Yoshimura, S. Suzuki, *Inorg. Chim. Acta* **1988**, *152*, 241.
[51] a) J. H. Dawson, *Science* **1988**, *240*, 433; b) T. L. Poulus, *J. Biol. Inorg. Chem.* **1996**, *1*, 356; c) D. B. Goodin, *J. Biol. Inorg. Chem.* **1996**, *1*, 360; d) S. Franzen, M. P. Roach, Y.-P. Chen, R. B. Dyer, W. H. Woodruff, J. H. Dawson, *J. Am. Chem. Soc.* **1998**, *120*, 4658.
[52] a) C. J. Hanke, J. G. Drewett, C. R. Myers, W. B. Campbell, *Endocrinology* **1998**, *139*, 4053; b) K. del Punta, E. H. Charreau, O. Pignataro, *Endocrinology* **1996**, *137*, 5337.
[53] a) R. E. Ebel, D. H. O'Keeffe, J. A. Peterson, *FEBS Lett.* **1975**, *55*, 198; b) D. H. O'Keeffe, R. E. Ebel, J. A. Peterson, *J. Biol. Chem.* **1978**, *253*, 3509.
[54] S. Hu, J. R. Kincaid, *J. Am. Chem. Soc.* **1991**, *113*, 2843.
[55] a) G. B. Richter-Addo, R. A. Wheeler, C. A. Hixson, L. Chen, M. A. Khan, M. K. Ellison, C. E. Schulz, W. R. Scheidt, *J. Am. Chem. Soc.* **2001**, *123*, 6314; b) S. A. Roberts, A. Weichsel, Y. Qiu, J. A. Shelnutt, F. A. Walker, W. R. Montfort, *Biochemistry* **2001**, *40*, 11327; c) M. K. Ellison, C. E. Schulz, W. R. Scheidt, *J. Am. Chem. Soc.* **2002**, *124*, 13833.
[56] D. J. Taube, H. D. Projahn, R. van Eldik, D. Magde, T. G. Traylor, *J. Am. Chem. Soc.* **1990**, *112*, 6880.
[57] C. Jung, N. Bec, R. Lange, *Eur. J. Biochem.* **2002**, *269*, 2989.
[58] a) S. C. Tang, S. Koch, G. C. Papaefthymiou, S. Foner, R. B. Frankel, J. A. Ibers, R. H. Holm, *J. Am. Chem. Soc.* **1976**, *98*, 2414; b) C. Caron, A. Mitschler, G. Riviere, L. Ricard, M. Schapacher, R. Weiss, *J. Am. Chem. Soc.* **1979**, *101*, 7401; c) H. Ogoshi, H. Sugimoto, Z. Yoshida, *Tetrahedron Lett.* **1975**, *16*, 2289.
[59] T. Higuchi, S. Uzu, M. Hirobe, *J. Am. Chem. Soc.* **1990**, *112*, 7051.
[60] a) T. Higuchi, K. Shimada, N. Maruyama, M. Hirobe, *J. Am. Chem. Soc.* **1993**, *115*, 7551; b) Y. Urano, T. Higuchi, M. Hirobe, T. Nagano, *J. Am. Chem. Soc.* **1997**, *119*, 12008; c) T. Higuchi, M. Hirobe, *J. Mol. Catal. A* **1996**, *113*, 403.
[61] N. Suzuki, T. Higuchi, Y. Urano, K. Kikuchi, T. Uchida, M. Mukai, T. Kitagawa, T. Nagano, *J. Am. Chem. Soc.* **2000**, *122*, 12059.
[62] A. Franke, G. Stochel, N. Suzuki, T. Higuchi, K. Okuzono, R. van Eldik, *J. Am. Chem. Soc.* **2005**, *127*, 5360.
[63] D. Zheng, R. L. Birke, *J. Am. Chem. Soc.* **2002**, *124*, 9066.
[64] F. A. Walker, *J. Inorg. Biochem.* **2005**, *99*, 216.
[65] a) W.-D. Woggon, T. Leifels, L. Sbaragli, *Cytochromes P450: Biochemistry Biophysics and Drug Metabolism*, International Conference on Cytochromes P450, 13th, Prague, Czech Republic, June 29-July 3; b) D. N. Meyer, W.-D. Woggon, *Chimia* **2005**, *59*, 85; c) W.-D. Woggon, *Acc. Chem. Res.* **2005**, *38*, 127; d) S. Kozuch, T. Leifels, D. Meyer, L. Sbaragli, S. Shaik, W.-D. Woggon, *Synlett* **2005**, *4*, 675; e) L. Sbaragli, W.-D. Woggon, *Synthesis* **2005**, *9*, 1538; f) D. Meyer, T. Leifels, L. Sbaragli, W.-D. Woggon, *Biochem. Biophys. Res. Commun.* **2005**, *338*, 372.
[66] N. Hessenauer-Ilicheva, A. Franke, D. Meyer, W.-D. Woggon, R. van Eldik, manuscript in preparation.
[67] A. Franke, N. Hessenauer-Ilicheva, D. Meyer, G. Stochel, W.-D. Woggon, R. van Eldik, *J. Am. Chem. Soc.* **2006**, *128*, 13611.
[68] a) J. C. W. Chien, *J. Am. Chem. Soc.* **1969**, *91*, 2166; b) A. Ehrenberg, T. W. Szczepkowski, *Acta Chem. Scand.* **1960**, *14*, 1.
[69] a) A. J. Gow, B. P. Luchsinger, J. R. Pawloski, D. J. Singel, J. S. Stamler, *Proc. Natl. Acad. Sci. USA* **1999**, *96*, 9027; b) V. S. Sharma, R. A. Isaacson, M. E. John, M. R. Waterman, M. Chevion, *Biochemistry* **1983**, *22*, 3897; c) A. W. Addison, J. J. Stephanos, *Biochemistry* **1986**, *25*, 4104.
[70] M. Hoshino, M. Maeda, R. Konishi, H. Seki, P. C. Ford, *J. Am. Chem. Soc.* **1996**, *118*, 5702.
[71] a) D. Tran, B. W. Skelton, A. H. White, L. E. Laverman, P. C. Ford, *Inorg. Chem.* **1998**, *37*, 2505; b) K. M. Miranda, R. W. Nims, D. D. Thomas, M. G. Espay, D. Citrin, M. D. Bartberger, N. Paolocci, J. M. Fukuto, M. Feelisch, D. A. Wink, *J. Inorg. Biochem.* **2003**, *93*, 52; c) P. C. Ford, B. O. Fernandez, M. D. Lim, *Chem. Rev.* **2005**, *105*, 2439 and references cited therein; d) M. D. Lim, I. M. Lorkovic, P. C. Ford, *J. Inorg. Biochem.* **2005**, *99*, 151 and references cited therein.
[72] a) B. O. Fernandez, P. C. Ford, *J. Am. Chem. Soc.* **2003**, *125*, 10510; b) B. O. Fernandez, I. M. Lorkovic, P. C. Ford, *Inorg. Chem.* **2003**, *42*, 2; c) B. O. Fernandez, I. M. Lorkovic, P. C. Ford, *Inorg. Chem.* **2004**, *43*, 5393.
[73] J.-E. Jee, R. van Eldik, *Inorg. Chem.* **2006**, *45*, 6523.
[74] a) L. G. Rochelle, S. J. Morana, H. Kruszyna, M. A. Russell, D. E. Wilcox, R. P. Smith, *J. Pharmacol. Exp. Ther.* **1995**, *275*, 48; b) M. Brouwer, W. Chamulitrat, G. Ferruzi, D. L. Sauls, J. B. Weinberg, *Blood* **1996**, *88*, 1857; c) S. S. Greenberg, J. M. Xie, D. R. Kapusta, M. J. S. Miller, *J. Pharmacol. Exp. Ther.* **1995**, *273*, 257; d) D. Zheng, R. Birke, *J. Am. Chem. Soc.* **2001**, *123*, 4637; e) H. Kruszyna, J. S. Magyar, L. G. Rochelle, M. A. Russell, R. P. Smith, *J. Pharmacol. Exp. Ther.* **1998**, *285*, 665.
[75] M. Wolak, G. Stochel, M. Hamza, R. van Eldik, *Inorg. Chem.* **2000**, *39*, 2018.
[76] C. Selcuki, R. van Eldik, T. Clark, *Inorg. Chem.* **2004**, *43*, 2828.
[77] V. S. Sharma, R. B. Pilz, G. R. Boss, D. Madge, *Biochemistry* **2003**, *42*, 8900.
[78] M. Wolak, A. Zahl, T. Schneppensieper, G. Stochel, R. van Eldik, *J. Am. Chem. Soc.* **2001**, *123*, 9780.
[79] L. E. Laverman, *PhD Dissertation*, University of California Santa Barbara, USA, **1999**.
[80] F. Roncaroli, R. van Eldik, *J. Am. Chem. Soc.* **2006**, *128*, 8042.
[81] a) E. Fujita, J. Fajer, *J. Am. Chem. Soc.* **1983**, *105*, 6743; b) S. Kelly, D. Lancon, K. M. Kadish, *Inorg. Chem.* **1984**, *23*, 1451; c) E. Fujita, C. K. Chang, J. Fajer, *J. Am. Chem. Soc.* **1985**, *107*, 7665; d) K. M. Kadish, X. H. Mu, X. Q. Lin, *Inorg. Chem.* **1988**, *27*, 1489; e) X. H. Mu, K. M. Kadish, *Inorg. Chem.* **1990**, *29*, 1031; f) S. Cheng, Y. O. Su, *Inorg. Chem.* **1994**, *33*, 5847.
[82] a) J. Abwao-Konya, A. Cappelli, L. Jacobs, M. Krishnamurthy, M. Smith, *Transition Met. Chem.* **1984**, *9*, 270; b) K. R. Ashley, J. G. Leipoldt, *Inorg. Chem.* **1981**, *20*, 2326; c) K. R. Ashley, S. Au-Young, *Inorg. Chem.* **1976**, *15*, 1937; d) R. F. Pasternack, M. A. Cobb, N. Sutin, *Inorg. Chem.* **1975**, *14*, 866; e) R. F. Pasternack, M. A. Cobb, *J. Inorg. Nucl. Chem.* **1973**, *35*, 4327;

f) R. K. Ashley, M. Berggren, M. Cheng, *J. Am. Chem. Soc.* **1975**, *97*, 1422; g) R. F. Pasternack, G. R. Parr, *Inorg. Chem.* **1976**, *15*, 3087; h) J. G. Leipoldt, R. van Eldik, H. Kelm, *Inorg. Chem.* **1983**, *22*, 4146.
[83] F. Roncaroli, T. E. Shubina, T. Clark, R. van Eldik, *Inorg. Chem.* **2006**, *45*, 7869.
[84] a) M. S. A. Hamza, X. Zou, K. L. Brown, R. van Eldik, *Eur. J. Inorg. Chem.* **2003**, 268; b) M. S. A. Hamza, R. van Eldik, *Dalton Trans.* **2004**, 1.

Received: September 29, 2006
Published Online: February 2, 2007

